

DISCRETE-CONTINUOUS HIGH-DIMENSIONAL DYNAMIC OPTIMIZATION[‡]

LORETTI I. DOBRESCU* AND AKSHAY SHANKER[†]

ABSTRACT. We provide a rigorous and unified foundation of the Euler equation and the Endogenous Grid Method (EGM) for a general multidimensional stochastic dynamic optimization problem with discrete and continuous states, non-smooth constraints, unbounded rewards, and non-compact feasibility correspondences. Our contribution is threefold. First, we provide a real-valued analogue to the Hamiltonian used to (painlessly) recover the necessary Euler equation for *any* stochastic dynamic optimization application. Second, we provide the necessary and sufficient conditions on model primitives that determine the invertibility of the Euler equation, and geometric structure of the exogenous grid. Third, we present a general, computationally efficient, user-friendly ‘rooftop-cut’ algorithm to compute the upper envelope of the value correspondence generated by EGM in discrete-continuous models. The algorithm asymptotically recovers the optimal solution and provides error bounds under standard assumptions. Finally, we illustrate our contributions with two workhorse applications tackling retirement choice and savings, and housing investments under frictions.

Key Words: discrete and continuous choices, non-convex optimization, Euler equation, dynamic programming

JEL Classification: C13, C63, D91

* Corresponding author. School of Economics, University of New South Wales, Sydney 2052 Australia. Email: dobrescu@unsw.edu.au.

[†] School of Economics, University of New South Wales, Australia and ARC Center for Excellence in Population Ageing Research (CEPAR), Sydney 2052 Australia. Email: a.shanker@unsw.edu.au.

[‡] We thank Max Blesch, Chris Carroll, Mateo Velasquez-Giraldo, Greg Kaplan, Sebastian Gsell, Mike Keane, Anant Mathur, Adrian Monninger, Lucas Pahl, and John Stachurski for valuable discussions and comments. Research support from the Australian Research Council (ARC LP150100608) and ARC Centre of Excellence in Population Ageing Research (CE17010005) is gratefully acknowledged. This research was undertaken with the assistance of resources and services from the National Computational Infrastructure (NCI), which is supported by the Australian Government. The software implementing the RFC algorithm and the applications can be found [here](#). All the proofs associated to the theoretical results are provided in the online appendix [here](#).

1. INTRODUCTION

Stochastic dynamic optimization has become one of the primary tools used by quantitative researchers in economics, finance, decision theory, and AI to characterize behavior across time. In such problems, today’s decisions affect the payoffs today but also the payoffs and constraints faced by an agent in the future (Bertsekas, 2022; Stachurski, 2022). To solve these models, dynamic programming provides us with a general computational procedure (i.e., the value function iteration - VFI) that does not require assumptions on the convexity and smoothness of the payoffs and constraints. A drawback of VFI, however, is that it relies on numerical optimization to iterate on the Bellman equation. In richer, more realistic models that demand high-dimensional state spaces, the grid size on which VFI iterates grows exponentially with each added state due to the curse of dimensionality (Rust, 1996).¹ As the grid size of an application increases, it is either inefficient or practically impossible to use VFI to solve the problem.

In practice, significant computational efficiency and accuracy can be gained by solving the first order condition (FOC) - or Euler equation - of the dynamic optimization problem. A popular approach based on the Euler equation combines policy iteration or Coleman-Reffett iteration (Coleman, 1990; Reffett, 1996) with EGM (Carroll, 2006).² In contrast to VFI or standard policy iteration that solve for the optimal end-of-period state (or ‘post-state’) given the current period state (Hull, 2015), EGM inverts the Euler equation on the post-state. In doing so, it can successfully eliminate costly numerical optimization (Iskhakov, 2015).³

An added issue to realistic applications becoming increasingly high-dimensional is that they also oftentimes involve both discrete choices and occasionally binding constraints.⁴ Discrete choices, occasionally binding constraints, and dimensionality present three crucial challenges to employing EGM. First, discrete choices introduce non-convexity into the problem, which can lead to multiple sub-optimal solutions to the Euler equation. In this case, the Euler equation will not be sufficient to recover the optimal policy. Second, in the presence of occasionally binding constraints (such as liquidity constraints), policy functions may not be differentiable everywhere. This precludes the use of standard envelope condition arguments to differentiate the value function. Existing results that

¹The high-dimensional economics literature is as large as it is varied, but it ultimately spans two categories of problems. First, high dimensionality arises when the agent chooses a number of quantities - for instance, where the decision space is related to the household portfolio allocation across assets (Kaplan et al., 2020) or to multi-product decisions (Midrigan, 2011). Second, it also arises when a number of different agents are modeled, possibly interacting via equilibrium prices such as, for instance, in Krusell and Smith (1998).

²Other methods that use FOCs include the envelope condition method (Maliar and Maliar, 2013; Arellano et al., 2016), and deep learning methods that minimize the Euler equation error (Maliar et al., 2021a). While here we present our ‘rooftop-cut’ (RFC) algorithm for EGM, this approach and our theoretical results carry over to any solution method that uses FOCs to retrieve optimal solutions in discrete-continuous optimization problems.

³Other approaches to resolve the numerical implications of high-dimensionality include using sparse grids (e.g., Brumm and Scheidegger (2017)) or improve the methods to arrive at and approximate the stationary policy in infinite horizon models (e.g. Maliar et al. (2021b) and Auclert et al. (2021)). Our work complements these approaches by focusing on the within period solution step.

⁴For instance, in models used to understand frictions (Skiba, 1978; Rust, 1987; Khan and Thomas, 2008; Kaplan and Violante, 2014; Dobrescu et al., 2018; Attanasio et al., 2018; Kaplan et al., 2020), the dynamics of housing stock adjustments (Yogo, 2016; Fagereng et al., 2019), asset pricing in the presence of frictions (Cooper, 2006), or the effect of mortgage refinancing on life-cycle asset allocation (Laibson et al., 2021).

generalize the Euler equation (i) do not accommodate occasionally binding constraints (González-Sánchez and Hernández-Lerma, 2013), or (ii) rely on restrictive assumptions (i.e., boundedness and compactness) on the reward functions and feasibility correspondences (Rincón-Zapatero and Santos, 2009; Rendahl, 2015) to ensure value function differentiability. Such assumptions are, however, violated in more realistic applications (Carroll and Shanker, 2024), and so far, results that accommodate unbounded rewards, for instance, remain model-specific (Li and Stachurski, 2014; Ma et al., 2022; Carroll and Shanker, 2024). Finally, when solving stochastic models with multiple states and choices, one does not know what conditions (that can be easily verified) are required for the EGM procedure to be well-defined - i.e., when can the Euler equation that takes into account the optimal constraint choice be inverted, and what is the geometric structure of the space of variables on which it can be inverted.

We resolve these three issues within the unified framework of an inverse dynamic optimization problem (Iyengar and Kang, 2005; Gonzalez-Sanchez and Hernandez-Lerma, 2013; Chan et al., 2023).⁵ Our first contribution is to prove the necessity of a generalized Euler equation that can be applied to any multidimensional stochastic dynamic optimization model, without the restrictions mentioned above. The approach we take is to characterize the Euler equations using a real-valued perturbation function, a discrete time analogue to a stochastic Hamiltonian – the ‘S-function’. The S-function represents the change in the objective function value given a time-, state- and information-specific perturbation of the current period state. To circumvent the need to directly differentiate the value function, we prove the necessity of the Euler equation by applying variational arguments on the Hilbert space of random variables generated by feasible policies. Importantly for more complex applications, the differentiation of the S-function can be defined in terms of real-valued calculus on the model primitives, and the first conditions can then be used to recover the Euler equation without the need for cumbersome envelope conditions or abstract functional derivatives.

Second, we develop a formal theory of the EGM as an inverse optimization problem defined on the joint space of post-states and intratemporal Kuhn-Tucker multipliers associated with the constraints - i.e., the space of ‘observable variables’. We provide necessary and sufficient conditions for ‘pure EGM’, a situation when the Euler equation for the unconstrained solution can be inverted (analytically or numerically) on the post-state space. In particular, the Hessian of the S-function with respect to the current period state must have the same rank as the dimension of the exogenous grid. Remarkably, invertibility of ‘pure EGM’ depends only on the dimensionality of the states and observable variables, and on the curvature of model primitives – i.e., the reward, transition, and constraint functions; it does not depend on the (harder to verify) curvature of the policy or value functions. The reason behind this result is that knowing the expectation of the marginal value of future states, the information one needs to compute the current period state is contained in the *value* of the post-state, and the current reward and transition functions (Carroll, 2006). On the other hand, when ‘pure EGM’ cannot be applied, the expected shadow values of future states

⁵In the context of dynamic programming, inverse problems have been formulated using Euler equations to solve the problem of recovering model parameters from observed policies. Our paper notes that the definition of an inverse problem is also a natural way to formulate the EGM.

will determine the structure of the exogenous grid. In this case, we provide conditions on the policy function (i.e., local injectivity and continuity) guaranteeing that the Euler equation can be inverted from a reduced-dimensional subset of the observable space. Numerical root-finding can then be used to construct the exogenous grid and EGM can still be used to gain computational efficiency over VFI. A key implication of our theory is thus that it enables EGM to be robustly employed in models (with or without discrete choices) where an analytical inverse to the Euler equation may not exist.

Finally, we present an off-the-shelf, computationally efficient, accurate, and user-friendly algorithm to compute the upper envelope of the value correspondence generated by EGM, and obtain the optimal policy function for dynamic programming problems with both discrete and continuous choices. The algorithm, dubbed ‘rooftop-cut’ (or RFC), works by noting that the upper envelope of the value correspondence is the supremum of choice-specific concave value functions, with each value function corresponding to a history-dependent future sequence of discrete choices. The convex regions of the upper envelope occur where different choice-specific value functions cross (and generate ‘kink points’), with the optimal policy function experiencing discontinuous jumps only in these regions. As a result, the algorithm checks each point of the endogenous grid to see if the tangent to the future choice-specific value function at that point dominates neighboring points. If a neighboring point is dominated and moving to it induces a jump in the policy function, then this point is removed. If a neighbouring point dominates the tangent, a first order approximation of the kink point is added to the endogenous grid. The RFC algorithm has the significant advantage that it can be easily programmed using vectorized (array) operations, making it particularly compatible with high-performance computing infrastructure and programming languages. A further advantage of our algorithm is its ability to recover the upper envelope without tying it to a particular interpolation method on the irregular multidimensional grid.

Last but definitely not least, we also provide a point-wise asymptotic error bound for both the RFC algorithm and EGM without discrete choices, under standard economic assumptions. These assumptions only relate to the Lipschitz continuity of the policy functions,⁶ and the monotonicity of the policy function holding the future sequence of discrete choices fixed. A corollary is that moments generated by simulation of policies solved using the generalized Euler equation and RFC (or EGM without discrete choices) are asymptotically accurate as the grid size is refined.

We use two foundational applications to illustrate the key contributions of the paper. As a benchmark, we first study a model of liquid and illiquid (i.e., financial and pension) savings in the presence of an absorbing retirement choice *a’ la* Druedahl and Jørgensen (2017). In this case, we show how the Euler equation derived using the S-function can be used to determine the optimal binding constraints given a point in the exogenous grid, avoiding any further numerical loops to optimize over the constraint choices. Owing to the time efficiency of our RFC method, we are able to use a standard SCIPY implementation of Delaunay triangulation in PYTHON to optimally interpolate

⁶Most economic applications feature bounded marginal propensities to consume and save, implying Lipschitz behavior. While a key RFC advantage is that it does not require monotonicity of the policy function, the agents problem holding future choices fixed is a concave problem with standard monotonicity (White, 2015).

the policy function. Compared to the upper envelope method in Druedahl and Jørgensen (2017), the combination of our RFC algorithm with Delaunay triangulation is (i) as fast as Druedahl and Jørgensen (2017), both methods being two orders of magnitude faster than VFI, and (ii) slightly more accurate, with accuracy gains arising because we are using first order information to ‘delete’ sub-optimal points. Second, we examine a portfolio allocation problem where previous discrete-continuous EGM methods fail due to the non-monotonicity of the policy functions and an irregular exogenous grid. Featuring both liquid and illiquid (i.e., financial and housing) savings, this example also shows how an exogenous grid can be constructed by finding numerical roots of the shadow value function even though the Euler equation is not analytically invertible on the full-dimensional post-state space. Compared to VFI, we again find RFC with EGM is two orders of magnitude faster and more accurate. Moreover, compared to previous attempts to solve this type of problems, which use an EGM step nested within numerical optimization (Druedahl, 2021), we find up to an order of magnitude improvement in accuracy (in terms of the relative Euler error) and a 25% gain in computational speed.

Our paper advances considerably the latest dynamic programming methods to characterize and solve discrete-continuous dynamic models. In relation to the theoretical foundations of dynamic optimization (Sorger, 2015; Rincón-Zapatero and Santos, 2009; Li and Stachurski, 2014; Rendahl, 2015; Ma et al., 2022; Stachurski, 2022), we are the first to provide results on the necessity and sufficiency of the generalized Euler equation that can accommodate occasionally binding constraints, discrete choices, unbounded rewards, and non-compact feasibility correspondences. On the topic of computational methods using EGM (Carroll, 2006; White, 2015; Ludwig and Schön, 2018; Lujan, 2023), we are the first to provide (i) verifiable error bounds, (ii) the necessary and sufficient conditions for the EGM to be well-defined, and (iii) the conditions that characterize the geometric structure of the exogenous grids. Finally, for the implementation of EGM in applications with both discrete and continuous choices (Fella, 2014; Iskhakov et al., 2017; Druedahl and Jørgensen, 2017; Druedahl, 2021), our RFC algorithm is the first method that (i) does not require regularity of the exogenous grid or monotonicity of the optimal policy, (ii) is asymptotically guaranteed to approximate the optimal solution, and (iii) allows high-dimensional discrete-continuous models to exploit the massive parallelism of modern high performance computing infrastructure (e.g., GPUs).

The paper proceeds as follows. Section 2 introduces the setup of a general dynamic programming problem, and discusses the EGM challenges identified in the literature. Section 3 introduces the S-function and proves the necessary FOCs. Section 4 formalizes the EGM as an inverse dynamic optimization problem, provides necessary and sufficient conditions for the invertibility of the Euler equations, and introduces the RFC algorithm with its convergence properties. Section 5 provides two applications of the theory, together with an analysis of the computational accuracy and speed gains of our method compared to previous ones. Section 6 concludes.

2. GENERAL SETUP AND PRELIMINARY CONSIDERATIONS

2.1. Notation. To aid readability, in what follows we will use *italic* to denote variables, roman fonts for functions, and capital letters for spaces - e.g., at time t , y_t is a variable in the post-decision

state (or ‘post-state’) space Y_t with $y_t \in Y_t$, and y_t is the post-state policy function.⁷ Additionally, we use (i) bold letters with a $\vec{}$ superscript to denote a sequence of variables across time - e.g., $\vec{y}_t = \{y_t, y_{t+1}, \dots, y_T\}$ with T the terminal period of the dynamic programming problem, and (ii) capital calligraphic letters for a sequence of grid points labelled with superscript $\#$ - e.g., $\mathcal{Y}_t = \{y_{t,0}^\#, \dots, y_{t,N}^\#\}$ is a grid of N post-state points at time t with $\mathcal{Y}_t \subset Y_t$.

For clarity, we also note the following mathematical conventions used below. We use $\|\cdot\|$ to denote the Euclidean norm. For a set $S \subset \mathbb{R}^n$, S° refers to its interior, and for $x \in \mathbb{R}^n$, $\mathbb{B}_\epsilon(x)$ refers to the ϵ -ball about x . For an $m \times n$ matrix \mathbf{A} and $n \times p$ matrix \mathbf{B} , \mathbf{AB} denotes the matrix product. When \mathbf{B} is also an $m \times n$ matrix, $\mathbf{A} \circ \mathbf{B}$ will denote the Hadamard or pointwise product. For two euclidean column vectors a and b , we use $a \cdot b$ to denote the inner-product. For a function $f: \mathbb{R}^n \times \mathbb{R}^k \rightarrow \mathbb{R}^m$, partial derivatives and the Jacobian with respect to the argument x are denoted using $\partial_x f(x, y)$. Moreover, letting $f = (f_1, \dots, f_m)$, the Jacobian can be written as $\partial_x f(x, y) = [\nabla_x f_1(x, y), \dots, \nabla_x f_m(x, y)]^\top$, where $\nabla_x f_1(x, y)$ denotes gradient column vectors and \top denotes the matrix transpose.

Finally, (i) $\pi_Y: X \times Y \rightarrow Y$ denotes a projection operator defined by the evaluation $\pi_Y(x, y) = y$, and (ii) fixing $x^* \in X$, we use $\text{em}_Y: Y \rightarrow X \times Y$ to denote the embedding $y \mapsto (x^*, y) = \text{em}_Y(y)$.

2.2. The general dynamic optimization problem setup. We start by setting up a generic reduced form dynamic optimization problem⁸ that is consistent with the recent literature (Hernandez-Lerma and Lasserre, 2012; Hull, 2015; Ma et al., 2022; Sargent and Stachurski, 2023), but also explicitly incorporates discrete actions and states (Druehl and Jørgensen, 2017).

Let t index time, and assume $t \in \{0, \dots, T\}$, where $T \in \mathbb{N} \cup \{\infty\}$. For each t , the dynamic programming problem consists of the following:

- (1) A state space $X_t = W_t \times Z_t \times M_t$, where:
 - (i) W_t is an exogenous shock space, with $W_t \subset \mathbb{R}^{N_W}$,
 - (ii) Z_t is a discrete state space, with $Z_t \subset \mathbb{R}^{N_Z}$, and
 - (iii) M_t is a continuous state space, with $M_t \subset \mathbb{R}_+^{N_M}$.
- (2) A W_t -valued stochastic recursive sequence $\{w_t\}_{t=0}^T$ of shocks, with a transition kernel F_t^w .⁹
- (3) An action space $D_t \times Y_t$, where:
 - (i) D_t is a discrete choice space, with $D_t \subset \mathbb{N}^{N_D}$, and

⁷To further streamline the main text, we will use italic to denote both (i) a random variable that realizes in the state and post-state space (‘history contingent plans’ - see Hernandez-Lerma and Lasserre (2012)), and (ii) the realized value of a random variable, as a state or post-state, at a given time - a distinction that is important when we prove our Euler equation results. A formal mathematical treatment is given in the online appendix, where we set up a stochastic sequence problem in a Hilbert space.

⁸Specifying the problem in reduced form without controls (Sorger, 2015) is without loss of generality.

⁹Without loss of generality, we can assume (i) $w_{t+1} = F_t^w(w_t, \eta_{t+1})$ for a measurable function F_t^w , where $\{\eta_t\}_{t=0}^T$ is a sequence of random variables defined on a common probability space $(\Omega, \Sigma, \mathbb{P})$, and (ii) w_0 is degenerate. Note that a stochastic recursive sequence (SRS) is more general than a Markov process - see Borovkov (2013) and Stachurski (2022).

- (ii) Y_t is a continuous post-state space, with $Y_t \subset \mathbb{R}^{N_Y}$.
- (4) A feasibility correspondence Γ_t , with $\Gamma_t: X_t \rightrightarrows D_t \times Y_t$, where $(d_t, y_t) \in \Gamma_t(x_t)$ if and only if $g_t(w_t, z_t, m_t, d_t, y_t) \geq 0$ for a concave measurable function g_t , with $g_t(w_t, z_t, \cdot, d_t, \cdot): \mathbb{R}^{N_M} \times \mathbb{R}^{N_Y} \rightarrow \mathbb{R}^{N_g}$ for each $(w_t, z_t, d_t) \in W_t \times Z_t \times D_t$.
- (5) A concave measurable reward function u_t , with $u_t: \text{Gr}\Gamma_t \rightarrow \mathbb{R} \cup \{-\infty\}$, where we write $u_t(w_t, z_t, m_t, d_t, y_t)$ as the evaluation of u_t .
- (6) A transition kernel F_t^m for the continuous state, with $F_t^m: D_t \times Y_t \times W_{t+1} \rightarrow M_{t+1}$, and a discrete transition kernel F_t^d , with $F_t^d: D_t \times W_{t+1} \rightarrow Z_{t+1}$.

Each period, the agent observes a state x_t , with $x_t \in X_t$, and responds with two actions: a feasible discrete choice $d_t \in D$, and a continuous post-state $y_t \in Y_t$ such that $(d_t, y_t) \in \Gamma_t(x_t)$. The agent obtains a reward $u_t(w_t, z_t, m_t, d_t, y_t)$ and moves to the next period random state x_{t+1} , where $x_{t+1} = (w_{t+1}, z_{t+1}, m_{t+1})$ and

$$(1) \quad x_{t+1} = F_t(d_t, y_t, w_{t+1})$$

with F_t denoting the tuple (F_t^w, F_t^d, F_t^m) .

The agent solves for a sequence of measurable policy functions $\{d_t, y_t\}_{t=0}^T$, where $d_t: X_t \rightarrow D_t$ and $y_t: X_t \rightarrow Y_t$ for each t . Given the initial state $x_0 \in X_0$, the value function $v_0: X_0 \rightarrow \mathbb{R} \cup \{-\infty\}$ becomes

$$(DP) \quad v_0(x_0) = \sup_{\{d_t, y_t\}_{t=0}^T} \mathbb{E}_{x_0} \sum_{t=0}^T u_t(w_t, z_t, m_t, d_t(x_t), y_t(x_t))$$

such that (1) holds with $y_t = y_t(x_t)$ and $d_t = d_t(x_t)$ for each t , and $(d_t(x_t), y_t(x_t)) \in \Gamma_t(x_t)$ for each t and x_t – i.e., such a sequence $\{d_t, y_t\}_{t=0}^T$ of policy functions is feasible. The conditional expectation operator \mathbb{E}_{x_0} is conditional on the time $t = 0$ realization of the state. To maintain generality, we do not specify a particular structure of time discounting; following (Cosar and Green, 2014), u_t can be interpreted as a payoff discounted to $t = 0$.

Since our aim is to provide a general method to characterize and solve (DP), we assume for brevity that a solution to this problem exists. In practice, the existence of a solution can be verified using the recent methods outlined in the literature (Feinberg et al., 2012; Shanker, 2017; Ma et al., 2022; Carroll and Shanker, 2024).

Assumption 1. *There exists a sequence of feasible sequence of measurable policy functions $\{d_t, y_t\}_{t=0}^T$ such that $v_0: X_0 \rightarrow \mathbb{R}$ and*

$$(2) \quad v_0(x_0) = \mathbb{E}_{x_0} \sum_{t=0}^T u_t(w_t, z_t, m_t, d_t(x_t), y_t(x_t)) < \infty \quad x_0 \in X_0$$

Under Assumption 1, the Bellman equation for each v_t , conditional on time t information, becomes

$$(BE) \quad v_t(x_t) = \max_{d_t, y_t \in \Gamma_t(x_t)} \{u_t(w_t, z_t, m_t, d_t, y_t) + \mathbb{E}_{x_t} v_{t+1}(x_{t+1})\}, \quad x_t \in X_t$$

such that (1) holds. We can also write a current period discrete choice (‘current discrete choice’)-specific Bellman equation as

$$(3) \quad v_{d_t,t}(x_t) = \max_{y_t \in \Gamma_{d_t,t}(x_t)} \{u_t(w_t, z_t, m_t, d_t, y_t) + \mathbb{E}_t v_{t+1}(x_{t+1})\}, \quad x_t \in X_t$$

where $\Gamma_{d_t,t}$ denotes the set $\{y_t \mid d_t, y_t \in \Gamma_t(x_t)\}$, and we let $y_{d_t,t}$ denote the current discrete choice-specific policy function.

While we characterize the Euler equation of the problem in Section 3, the following notation will aid the discussion below:

Remark 1. *For each t , a sufficient and necessary Euler equation for the maximization problem in (3) is a function $\mathbf{E}_t: \mathbb{R}^{N_Y} \times \mathbb{R}^{N_g} \times \mathbb{R}^{N_M} \rightarrow \times \mathbb{R}^{N_Y} \times \mathbb{R}^{N_g}$ such that $\mathbf{E}_t(y_t, \mu_t \mid m_t) = 0$ if and only if y_t solves (3) given m_t and (w_t, z_t, d_t) .*

2.2.1. Fixed variables and active state space. The post-state policy functions are usually computed in applications given (i) a realization of an exogenous shock, and (ii) the values of the discrete state and of the current discrete choice. It will thus be useful to collect these ‘fixed’ variables in a tuple ξ_t , where $\xi_t = (w_t, z_t, d_t)$.

Furthermore, note that during computation, the dimensionality of the continuous state space can often be reduced.¹⁰ To formalize the dimensionality reduction in our general setting, we consider the problem to have an ‘active state representation’ if there exists (i) $\bar{M}_t \subset \mathbb{R}^{N_M}$ such that $\dim(\bar{M}_t) =: N_{\bar{M}} < N_M$, and (ii) continuous selection functions $\phi_t: M_t \rightarrow \bar{M}_t$ and $\bar{y}_t(\xi_t, \cdot): \bar{M}_t \rightarrow Y_t$ such that if $y_{d_t,t}$ is an optimal policy then $y_{d_t,t}(x_t) = \bar{y}_t(\xi_t, \phi_t(m_t))$ for all x_t and d_t . In what follows, when the fixed variables ξ_t are given, we will abbreviate $\bar{y}_t(\xi_t, \bar{m}_t)$ to $\bar{y}_t(\bar{m}_t)$, where the dependence of \bar{y}_t on ξ_t is implicit. We can similarly define the evaluation of the reward function and constraints on the active state space as $\bar{u}_t(\phi_t(m_t), y_t)$ and $\bar{g}_t(\phi_t(m_t), y_t)$, respectively.

2.3. Euler equation challenges. Before we turn to characterizing the Euler equation and its arguments, we detail three technical challenges that arise when computing the solution to the problem above using an Euler equation. First, the Euler equation may not be sufficient due to non-concavity of the value function generated by discrete choices. Second, the value function may not be differentiable everywhere due to discrete choices and occasionally binding constraints, precluding the use of standard envelope theorem methods to derive the necessary Euler equation.¹¹ Third, when employing EGM, one inverts the Euler equation by solving $m_t \mapsto \mathbf{E}_t(y_t, \mu_t \mid m_t) = 0$ for m_t over an exogenous grid in which y_t is held fixed. In this case, there is no formal theory of how to set up an exogenous grid such that the inverse of the Euler equation satisfying the occasionally binding constraints given by the constraint functions g_t is well-defined. We discuss each of these challenges next.

¹⁰See for instance Fella (2014), where in a model with two wealth states (i.e., liquid and housing assets), one overall wealth state becomes sufficient to compute the optimal policy for those who adjust housing stock.

¹¹See Stachurski (2022) for the standard use of the envelope conditions in smooth problems.

2.3.1. *Non-concavity and sufficiency of the Euler equation.* We start our discussion of the EGM challenges by formally explaining the reasons why the value function may not be concave in the presence of discrete choices. This formalization will also play a key role in the algorithm we present to remove sub-optimal points.

To begin, fix x_t and let $\vec{d}_t = \{d_j, \dots, d_T\}$ denote a stochastic sequence of discrete choices starting at time t and ending at time T , to which we refer to as ‘future discrete choices’. In particular, let $\{d_j, y_j\}_{j=t}^T$ be a sequence of discrete choice and post-state policy functions. Define the discrete choices and states generated under these policies as¹²

$$(4) \quad d_j = d_j(x_j), \quad x_j = F(d_j, y_j(x_j), w_{j+1})$$

Consider the future choice-specific dynamic programming problem

$$(CS-DP) \quad v_t^{\vec{d}_t}(w_t, z_t, m_t) := \max_{\{y_j\}_{j=t}^T} \mathbb{E}_0 \sum_{j=0}^T u_j(w_j, z_j, m_j, d_j, y_j(x_j)),$$

such that (1) holds. Since the stochastic sequence of future discrete choices \vec{d}_t remains fixed for each t , the problem becomes a standard concave dynamic optimization problem. Moreover, $v_t^{\vec{d}_t}(w_t, z_t, \cdot)$ will be a concave function. Next, let $\Gamma_{D,t}^T$ denote the correspondence defined on the X_t mapping to feasible future discrete choices starting at t , with¹³

$$(5) \quad \Gamma_{D,t}^T(x) := \left\{ \vec{d}_t \in \prod_t^T D_t \mid d_j, y_j \in \Gamma_j(x_j), \right. \\ \left. x_{j+1} = F_j(d_j, y_j, w_{j+1}), x_t = x, j = t, \dots, T \right\}$$

If $\vec{d}_t \in \Gamma_{D,t}^T(x_t)$, we will simply say \vec{d}_t is feasible given x_t . The Bellman equation for our original problem (BE) can now be written as

$$(BE-2) \quad v_t(x_t) = \max_{d_t, y_t \in \Gamma_t(x_t)} \left\{ u_t(w_t, z_t, m_t, d_t, y_t) + \max_{\vec{d}_{t+1}} \left\{ \mathbb{E}_t v_{t+1}^{\vec{d}_{t+1}}(w_{t+1}, z_{t+1}, m_{t+1}) \right\} \right\} \\ = \max_{d_t, y_t \in \Gamma_t(x_t)} \max_{\vec{d}_{t+1}} \underbrace{\left\{ u_t(w_t, z_t, m_t, d_t, y_t) + \mathbb{E}_t v_{t+1}^{\vec{d}_{t+1}}(w_{t+1}, m_{t+1}) \right\}}_{=: Q_t^{\vec{d}_{t+1}}(x_t, d_t, y_t)}$$

such that \vec{d}_{t+1} is feasible given x_{t+1} , and (1) holds. Even if we hold d_t and d_{t+1} fixed, the next period value function v_{t+1} will not be concave in the continuous state. This is because the max operator over the non-convex set $\Gamma_{D,t+1}^T(x_{t+1})$ does not commute concavity, and v_{t+1} is the upper envelope over a sequence of feasible future discrete choices. Figure 1 illustrates this situation by showing v_t as the upper envelope of the concave functions $v_t^{\vec{d}_t}(w_t, z_t, \cdot)$, where each of these concave functions is a value function conditional on a *sequence* of future discrete choices. Thus, even with

¹²The sequence $\{d_j, x_j\}_{j=t}^T$ will be progressively measurable with respect to the filtration generated by the random variables $\{w_j\}_{j=t}^T$ with a realisation of w_t fixed.

¹³The feasible set of sequences of future discrete choices should be understood to contain sequences of random variables, while set relations and equalities in the definition of $\Gamma_{D,t}^T$ hold \mathbb{P} almost everywhere.

d_t held fixed, the optimization problem given by (3) remains non-concave. As such,

$$(6) \quad v_{d_t,t}(x_t) = \max_{y_t \in \Gamma_t(x_t)} Q_t(x_t, d_t, y_t),$$

where

$$(Q) \quad Q_t(x_t, d_t, y_t) = \max_{\vec{d}_{t+1}} Q_t^{\vec{d}_{t+1}}(x_t, d_t, y_t),$$

will not be concave. By controlling y_t in the Q function, we implicitly control the stochastic sequence of future discrete choices, leading to secondary kinks in the value function and discontinuous jumps in the policy function.

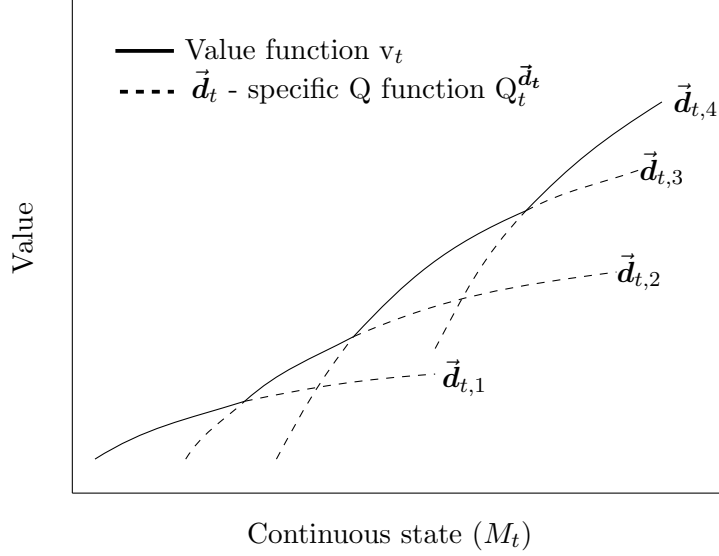


Figure 1. As function of the continuous state, the time t value function v_t is the upper envelope of concave functions, where each concave function is a value function conditional on a stochastic *sequence* of future discrete choices; the subscript i on $\vec{d}_{t,i}$ indicates distinct stochastic sequences of future discrete choices

The FOCs of the current choice-specific problem are thus not sufficient to characterize the optimal policy function since they do not select the optimal future sequence of discrete choices - or the upper envelope - in Figure 1. Importantly, when using EGM, we do not have access to all the possible $\vec{d}_{t,i}$ for any given continuous state m_t - we only have access to tuples $(m_t, y_t, v_t^{\vec{d}_{t+1}})$, where \vec{d}_{t+1} is optimal at $t+1$ if y_t is the end-of-period t post-state; we do not know whether \vec{d}_{t+1} is optimal given m_t .

The recent literature has proposed methods to determine the upper envelope of the future choice-specific value functions generated by EGM, which inverts the necessary FOCs. Two key limitations continue, however, to persist, namely (i) the inability of these algorithms to solve problems where both exogenous and endogenous grid points may be irregular or non-monotone (see application in Section 5.2.3, that cannot be solved using existing methods), and (ii) the lack of assurance (asymptotic or otherwise) that these methods are accurate for an arbitrary problem. Iskhakov et al. (2017)

introduces a method contingent on the monotonicity of the optimal policy that only accommodates ‘upward’ policy function jumps. This approach is demonstrated for a specific model, within a one-dimensional setting, and does not provide a theoretical indication of its precision or convergence. It also requires the exogenous grid to be regular, and only applies to cases where one can verify that the policy function is monotone, and the endogenous grid consists of clearly discernible monotone and connected segments.¹⁴ In contrast, Druedahl and Jørgensen (2017) offers a multidimensional algorithm that generates local triangulations on the endogenous grid by identifying triangles within the exogenous grid. The authors note that the points retrieved by their method become asymptotically dense in the optimal grid, but do not establish error bounds for approximations of the policy function. Furthermore, their method cannot be applied to settings where the exogenous grid is irregular, and it also relies on a particular interpolation and triangulation method. Doing so precludes using alternative interpolation methods such as Gaussian process regressions (Lujan, 2023) or Delauny triangulations (Chen and Xu, 2004), which may be more suitable for certain problems.¹⁵

2.3.2. Non-differentiability and necessity of the Euler equation. Figure 1 shows how the value function cannot be differentiable at the intersection points. Specifically, $v_t(x_t) = u_t(w_t, z_t, m_t, d_t, y_t(m_t)) + \mathbb{E}_t v_t(x_{t+1})$ and $x_{t+1} = F_t(d_t, y_t(m_t), w_{t+1})$, where y_t denotes the optimal policy function. If y_t exhibits a jump discontinuity due to a secondary kink at a given \hat{m}_t , then $\partial_m v_t$ will be undefined at \hat{m}_t because the left-hand side (LHS) and right-hand side (RHS) derivatives will not match (Iskhakov, 2015). Although Clausen and Strub (2020) characterize differentiability at locations other than the kink points,¹⁶ the implications for the Euler equation everywhere across the state space remain unexplored. Their method also requires analytically finding support functions, which may become cumbersome in complex applications.

Differentiability of the value function has been challenging even in the absence of discrete choices. In models with occasionally binding constraints, y_t will not be differentiable, and the standard envelope condition approach to derive the Euler equation will fail if optimal policies are not all in the interior of the feasible set. While progress has been made to characterize Euler equations in the presence of occasionally binding constraints, existing results require compact feasibility correspondences and, at the same time, do not allow the reward function to reach $-\infty$ (Rincón-Zapatero and Santos, 2009; Rendahl, 2015; Marimon and Werner, 2021). As a result, the existing results end up not accommodating quite a wide range of realistic reward functions. In particular, if feasibility correspondences are to be compact, then realistic constant relative risk aversion (CRRA)

¹⁴In models of non-durable stock accumulation with fixed adjustment costs, policy functions are not monotone and the exogenous grid is itself a subset of a lower-dimensional manifold of the post-state space, leading to irregularly spaced points; Section 5.2.3 elaborates. Another example of a method that requires monotonicity is Fella (2014).

¹⁵Delauny triangulations are the optimal triangulation that minimize the linear interpolation error on an irregular grid (Chen and Xu, 2004). While Druedahl and Jørgensen (2017) and Ludwig and Schön (2018) point out that Delaunay may come at significant computational cost, our numerical exercises show that using the appropriate software libraries can make Delaunay triangulations highly efficient without sacrificing the EGM speed advantage.

¹⁶Clausen and Strub (2020) prove a result indicating differentiability of the value function away from kink points, but under the assumption that the continuous choice is in the interior of the feasibility correspondence. Interiority is violated by many models, including our second application in Section 5 where a subset of the occasionally binding constraints actually end up binding (see Rincón-Zapatero and Santos (2009) and also Remark 7).

utility functions (i.e., with CRRA parameter above 1) in income fluctuation models, for instance, would require unbounded utility values that can reach $-\infty$ (Carroll and Shanker, 2024). While Li and Stachurski (2014) and Ma et al. (2022) derive the Euler equation without such restrictions,¹⁷ they only (i) focus on specific applications, and also (ii) assume bounded marginal utility and a strictly positive lower bound on income shocks. Moreover, these approaches cannot apply to models with a naturally arising liquidity constraint, such as models with unemployment risk (Carroll and Shanker, 2024).

All in all, a general ‘off-the-shelf’ theory to derive the Euler equation using standard real-valued calculus in the presence of discrete choices, multiple occasionally binding constraints, and unbounded reward functions has so far remained elusive.

2.3.3. Constraints and invertibility of the Euler equation. Even when discrete choices are set aside, there remains the open question of when the EGM is well-defined – i.e., what is the space of binding constraints and variables on which the Euler equation can be inverted. The answer to this question determines how to construct the exogenous grid and the set of constraints that bind given an EGM inverse solution. Iskakov (2015) gives conditions for when an analytical inverse of the Euler equation exists on the post-state space for problems without constraints. While Druedahl and Jørgensen (2017) points out that the policy functions must be an injection, it do not provide specific conditions that determine the structure of the exogenous grid on which invertibility holds. To deal with constraints, Druedahl and Jørgensen (2017) suggests evaluating the policy function using EGM for each possible constraint combination. The optimal policy function is then determined by an ‘outer loop’ that evaluates the value function on the state space for each constraint, and numerically chooses the optimal constraint. However, this outer loop leads to an unnecessary computational step that becomes costly in practical high-dimensional applications - such as Dobrescu et al. (2022) for instance. As we show in Section 4.1.1, the Euler equation sharply characterizes the exogenous grid on which an inverse exists, and the optimal constraints that bind given the implied state. This allows us to avoid any additional upper envelope loops by inverting only from the image of the policy function optimized over the constraint choice.

Finally, there are situations when an inverse does not exist on the full post-state space but an inverse of the Euler equation may exist on a lower-dimensional sub-space. In these cases, we will show that EGM can still be applied to gain computational efficiency and accuracy as in the application in Section 5.2.3.

3. THE EULER EQUATION

We now turn to our first main contribution and address the non-differentiability challenge identified above. After providing the general conditions required to prove the necessity of Euler equations, we introduce an S-function that can be used to easily derive FOCs even in the presence of discrete choices, occasionally binding constraints, and non-differentiability of the value function. We also show that a saddle point to the S-function is a sufficient and necessary condition for optimality given

¹⁷See also Dávila et al. (2012) and Cao (2020)

a stochastic sequence of future discrete choices, and then use the saddle point of the S-function to characterize Euler equations.

3.1. Main necessary and sufficient conditions. For the following assumptions, consider the setting of Assumption 1, and let $\{d_t, y_t\}_{t=0}^T$ be an optimal sequence of policy functions.

Assumption (D.1) For every $x_t \in X_t$ and $d_t \in D_t$, the function $u_t(w_t, z_t, \cdot, d_t, \cdot)$ is continuously differentiable on $\mathbb{B}_\epsilon(m_t, y_t)$ for some $\epsilon > 0$ and $y_t = y_t(x_t)$.

Assumption (D.2) For every $(w_t, z_t, d_t) \in W_t \times Z_t \times D_t$, the functions $g_t(w_t, z_t, \cdot, d_t, \cdot)$ and $F_t^m(d_t, \cdot, w_{t+1})$ are affine.

Assumption (D.3) For every $(w_t, z_t, m_t, d_t) \in W_t \times Z_t \times M_t \times D_t$, the Slater condition holds. That is, the set $\{y \mid g_t(w_t, z_t, m_t, d_t, y) > 0, g_t(w_{t+1}, z_{t+1}, m', d_{t+1}, y_{t+1}) > 0\}$ is non-empty, where $m' = F^m(d_t, y, w_{t+1})$ and $y_{t+1} = y_{t+1}(m_{t+1})$, $m_{t+1} = F^m(d_t, y_t(m_t), w_{t+1})$.

Assumptions D.1 - D.3 are unrestrictive (see Rincón-Zapatero and Santos (2009) for a detailed discussion). However, as mentioned above, our problem definition does not require that $u > -\infty$ or that Γ_t is compact-valued, and we do not impose a strictly positive lower bound on the marginal reward (i.e., utility) or value of the shocks. Importantly, we also allow for the presence of discrete choices.

To derive the necessary and sufficient FOCs, we consider instantaneous time t values of multipliers, which we define as the functions $\mu_t: X_t \rightarrow \mathbb{R}^{N_g}$ and $\Lambda_t: X_t \rightarrow \mathbb{R}^{N_M}$, and refer to their evaluation as ‘constraint multipliers’ and ‘shadow values of the state’, respectively. At the optimum, the constraint multipliers, evaluated at the current state, represent the marginal value of relaxing each inequality constraint. In turn, the shadow values of the state indicate the marginal value of increasing each state variable at the start of time t .

Fix $x_t \in X_t$, the discrete choice function d_t , the post-state policy function y_t , and a next period state shadow value function Λ_{t+1} . The S-function at time t is defined by

$$\begin{aligned} \text{(S)} \quad \mathbf{S}_t(m, y, \mu, \lambda \mid x_t, \Xi_t) : &= u_t(w_t, z_t, m, d_t, y) + \mathbb{E}_{x_t} \Lambda_{t+1}(x_{t+1}) \cdot F_t^m(d_t, y, w_{t+1}) \\ &\quad - \lambda \cdot m + \mu \cdot g_t(w_t, z_t, m, d_t, y) \end{aligned}$$

where $m \in M_t, y \in Y_t, \mu \in \mathbb{R}^{N_g}, \lambda \in \mathbb{R}^{N_M}$. To ease the notation, Ξ_t denotes the tuple of functions $(d_t, y_t, \Lambda_{t+1})$ and $m_{t+1} = F_t^m(d_t, y_t(x_t), w_{t+1})$, $z_{t+1} = F_t^d(d_t, w_{t+1})$, $w_{t+1} = F_t^w(w_t, \eta_{t+1})$, $x_{t+1} = (w_{t+1}, m_{t+1}, w_{t+1})$ and $d_t = d_t(x_t)$.

Analogous to a discrete time Hamiltonian, the S-function represents an incremental value of the objective function as a function of the state and post-state. In a stochastic discrete time setting, however, arguments for the Hamiltonian (or Lagrangian) become infinite-dimensional objects (Bewley, 1972; Dechert, 1982). Our innovation is to represent the multipliers, shadow value and incremental value as *functions* of the real-valued current state *holding expectations over the future fixed*. The formulation avoids differentiating the value function, and at the same time avoids the

use of abstract derivatives to compute the Euler equation. An immediate implication of using the S-function to derive the Euler equation is that it sharply characterizes the post-state and multiplier space in which constrained solutions exist (see Theorem 2 in the next section).

Our first main result tells us that if there exists a sequence of shadow value functions, non-negative constraint multipliers and policy functions such that m_t , $y_t(x_t)$, $\mu_t(x_t)$ and $\Lambda_t(x_t)$ are a saddle point of the S-function in the sense that

$$(7) \quad \partial_m \mathbf{S}_t(m_t, y_t(x_t), \mu_t(x_t), \lambda_t(x_t) \mid x_t, \Xi_t) = 0$$

$$(8) \quad \partial_y \mathbf{S}_t(m_t, y_t(x_t), \mu_t(x_t), \lambda_t(x_t) \mid x_t, \Xi_t) = 0$$

$$(9) \quad g_t(w_t, z_t, m, d_t, y_t(x_t)) \geq 0$$

$$(10) \quad \mu_t(x_t) \circ g_t(w_t, z_t, m, d_t, y_t(x_t)) = 0$$

then the post-state actions are optimal *given the sequence of future discrete states*. (Note the partial derivatives are taken holding the time subscripted variables of the S-function fixed.)

Let $\{d_t, y_t\}_{t=0}^T$ be a sequence of feasible policy functions, and let \vec{d}_0 and $\{m_t, y_t\}_{t=0}^T$ be generated by $\{d_t, y_t\}_{t=0}^T$.

Proposition 1. (Sufficient FOCs) Assume there exists a sequence $\{\mu_t\}_{t=0}^T$ and $\{\Lambda_t\}_{t=0}^T$ of measurable functions such that $\mu_t: X_t \rightarrow \mathbb{R}_+^{N_g}$ and $\Lambda_t: X_t \rightarrow \mathbb{R}_+^{N_M}$.

(1) If for every t and $x_t \in X_t$,

(i) m_t , $y_t(x_t)$, $\mu_t(x_t)$ and $\Lambda_t(x_t)$ are a saddle point of the S-function ((7) - (10) hold),

(ii) $\mathbb{E}_0 [\Lambda_{t+1}(x_{t+1}) F_t^m(d_t, y, w_{t+1})]^2 < \infty$, $\mathbb{E}_0 [\Lambda_{t+1}]^2 < \infty$, $\mathbb{E}_0 [\mu_t]^2 < \infty$, $\mathbb{E}_0 [m_t]^2$ and $\mathbb{E}_0 [y_t]^2 < \infty$, and

(iii) $T < \infty$ or $\lim_{t \rightarrow \infty} \mathbb{E}_0 [\Lambda_{t+1}(x_{t+1})] = 0$,

then $\{y_t\}_{t=0}^T$ solves (CS-DP) given \vec{d}_0 .

(2) In addition, if $d_t(x_t), \vec{d}_{t+1}, y_t(x_t) = \arg \max_{d, \vec{d}', y} Q_t^{\vec{d}'}(x_t, d, y)$ such that d, \vec{d}', y is feasible for

each t , then $\{d_t, y_t\}_{t=0}^T$ solves (DP).

Satisfying the FOCs (Item (1). of Proposition 1) is only a necessary condition for optimality in the sense of problem (DP). In the presence of non-convexity due to discrete choices, Item (2). of Proposition 1 must also hold. Item (2). says that each period, the entire future stochastic sequence of discrete choices implied by the post-state choice must be optimal. Note that, implicitly, the goal of upper envelope methods (Fella, 2014; Iskhakov et al., 2017; Druedahl and Jørgensen, 2017)) is to remove post-state values that do not satisfy Item (2).

Below we verify that any solution will be a saddle point to the S-function, which is the main result of Section 3.

Theorem 1. (Necessary FOCs) *If Assumption 1 and Assumptions D.1-D.3 hold, then there exists a measurable sequence $\{\mu_t\}_{t=0}^T$ and $\{\Lambda_t\}_{t=0}^T$, $\mu_t: X_t \rightarrow \mathbb{R}_+^{N_g}$ and $\Lambda_t: X_t \rightarrow \mathbb{R}_+^{N_M}$, such that for every t , m_t , $y_t(x_t)$, $\mu_t(x_t)$ and $\Lambda_t(x_t)$ are a saddle point of the S-function ((7) - (10) hold).*

For the following, let \vec{d}_t be generated $\{m_j, y_j\}_{t=j}^T$ by $\{d_j\}_{j=t}^T$.

Corollary 1. *If the conditions of Proposition 1 hold, then $v_t^{\vec{d}_t}(w_t, z_t, \tilde{m}_t) - v_t^{\vec{d}_t}(w_t, z_t, m_t) \leq \Lambda_t(x_t)(\tilde{m}_t - m_t)$ for all $m_t, \tilde{m}_t \in M_t$.*

It follows that while the value function may not be differentiable at the kink points (recall Section 2.3.2), the shadow value will be a sup-gradient and define a majorizing tangent plane to the value function conditional on a sequence of future discrete choices.¹⁸

3.2. The Euler equation in practice. Let us return to examining the FOCs of the S-function and how they are used in computation. Expanding (7) and (8), we have

$$\begin{aligned} \partial_m \mathbf{S}_t(m, y, \mu, \lambda | x_t, \Xi_t) &= \partial_m u_t(w_t, z_t, m, d_t, y) + \mu^\top \partial_m g_t(w_t, m, z_t, d_t, y) - \lambda^\top = 0 \\ \partial_y \mathbf{S}_t(m, y, \mu, \lambda | x_t, \Xi_t) &= \partial_y u_t(w_t, z_t, m, d_t, y) \\ &\quad + \mu^\top \partial_y g_t(w_t, z_t, m, d_t, y) + \mathbb{E} \Lambda_{t+1}(x_{t+1})^\top \partial_y F_t^m(d_t, y, w_{t+1}) = 0 \end{aligned}$$

In the above FOCs, x_{t+1} is a function of y_t , x_t and the shock w_{t+1} that we held fixed while differentiating the S-function.

By Proposition 1, sufficiency requires that given y_t , x_t and the expectation over the next period shock, a solution (m, y, μ, λ) to the above FOCs satisfies $y = y_t(x_t)$, $m = m_t$ and (10). Equivalently, given a time t state variable x_t , Λ_{t+1} and fixed variables ξ_t , the FOCs imply that an optimal solution is a feasible root to the generalized Euler equation $y, \mu, \lambda \mapsto \mathbf{E}_t^{\xi_t}(y, \mu, \lambda | m_t)$, defined by the following components:

$$(11) \quad \mathbf{E}_{m,t}^{\xi_t}(y, \mu, \lambda | m_t) = \partial_m u_t(w_t, z_t, m_t, d_t, y) + \mu^\top \partial_m g_t(w_t, z_t, m_t, y) - \lambda^\top$$

$$(12) \quad \mathbf{E}_{y,t}^{\xi_t}(y, \mu | m_t) = \partial_y u_t(w_t, z_t, m_t, d_t, y) \\ + \mu^\top \partial_y g_t(w_t, z_t, m_t, d_t, y) + \mathbb{E}_{x_t} \Lambda_{t+1}(x')^\top \partial_y F_t^m(d_t, y, w_{t+1})$$

$$(13) \quad \mathbf{E}_{\mu,t}^{\xi_t}(y, \mu | m_t) = \mu \circ g_t(w_t, z_t, m_t, d_t, y)$$

where $x' = (w_{t+1}, F_t^d(d_t, w_{t+1}), F_t^m(d_t, y, w_{t+1}))$, and such that $\mu > 0$. The Euler equation incorporates the intertemporal choice of the state (11), the intratemporal choice of the post-state (12), and the complementary slackness conditions associated with the constraints (13).

Following Iyengar and Kang (2005), we will refer to finding optimal values by finding roots to the Euler equation as the ‘forward problem’ – i.e., given Λ_{t+1} , one obtains optimal values of y_t, μ_t, λ_t for corresponding values of m_t and ξ_t to construct a policy function. Once the discrete choice function

¹⁸Formally, the shadow value will define a sup-differential to the value function (see online appendix). Under further restrictions on smoothness of model primitives, it is also possible to show that the conditional value function will be differentiable, however, differentiability is not needed for what follows.

d_t have also been computed (see below), the time t policy functions can be recovered. Equation (11) then defines the iteration of the vector of shadow value functions as follows:

$$(\mathbf{L}) \quad \Lambda_t(x_t) = \nabla_m \mathbf{u}_t(w_t, z_t, m_t, d_t(x_t), y_t(x_t)) + \nabla_m \mathbf{g}_t(w_t, m_t, d_t(x_t), y_t(x_t)) \mu_t(x_t),$$

and the time $t - 1$ policy functions can then be recovered given Λ_t

3.2.1. Computation of the forward problem using FOCs on the active state space. To detail the computation of the forward problem, without loss of generality, suppose there exists transformations of the functions \mathbf{u}_t and \mathbf{g}_t defined on an active state space \bar{M}_t . As such, let us define an ‘active forward problem’ that finds the roots of $(y, \mu, \lambda) \mapsto \bar{\mathbf{E}}_t(y, \mu, \lambda | \bar{m}_t)$, where

$$(\mathbf{EO1}) \quad \bar{\mathbf{E}}_{\bar{m},t}(y, \mu, \lambda | \bar{m}_t) := \partial_{\bar{m}} \bar{\mathbf{u}}_t(\bar{m}_t, y) + \mu_t^\top \partial_{m_t} \bar{\mathbf{g}}_t(\xi_t, \bar{m}_t, y) - \lambda^\top$$

$$(\mathbf{EO2}) \quad \bar{\mathbf{E}}_{y,t}(y, \mu | \bar{m}_t) := \partial_y \bar{\mathbf{u}}_t(\bar{m}_t, y) + \mu_t^\top \partial_y \bar{\mathbf{g}}_t(\xi_t, \bar{m}_t, y) + \mathbb{E} \Lambda_{t+1}(x')^\top \partial_y \mathbf{F}_t^m(d_t, y, w_{t+1})$$

$$(\mathbf{EO3}) \quad \bar{\mathbf{E}}_{\mu,t}(y, \mu | m_t) := \mu \circ \bar{\mathbf{g}}_t(w_t, z_t, m_t, d_t, y)$$

The computational procedure using Euler equations proceeds as follows:

- (A) Find the root of **(EO2)** given a continuous state \bar{m}_t and fixed variables. Typically, one finds the roots of $(y, \mu) \mapsto \bar{\mathbf{E}}_{y,t}(y, \mu | \bar{m}_t)$ such that $\bar{\mathbf{E}}_{\mu,t}(y, \mu | m_t) = 0$ via numerical methods or EGM.¹⁹
- (B) In the case of discrete-continuous problems, a method is used to select the optimal roots (i.e., the roots that satisfy Item (2). of Proposition 1). Once the optimal roots are found, the selection function ϕ_t can be used to construct the time t policy function $y_{dt,t}$. Equation **(EO1)** can then recover the shadow value $\lambda_{dt,t}$ as a function of the time t state and fixed variables.
- (C) The optimal *current period* discrete choices are computed by solving

$$d_t = \arg \max_{d, y_{d,t}(x_t) \in \Gamma_t(x_t)} v_t^d(x_t)$$

Once the current discrete choice function d_t has been computed, **(L)** can be used to recover λ_t .

To sum up, so far we (i) proved that the Euler equation is necessary to characterize optimality and also sufficient given a future sequence of discrete choices, and (ii) provided a straightforward way to derive the Euler equation in the presence of discrete choices and non-smooth constraints. With the Euler equations at hand, standard numerical root finding or EGM can then be used to implement the first step in the computational procedure just described above. However, the roots satisfying the FOCs are only sufficient to solve the dynamic programming problem given a future sequence of discrete choices. At any given time t , if the *entire future sequence of discrete choices*

¹⁹Evaluating the roots of $y, \mu \mapsto \bar{\mathbf{E}}_t^{\xi_t}(y, \mu | m_t)$ is equivalent to evaluating a policy under the Coleman-Reffett operator (Coleman, 1990; Reffett, 1996). Other foundational literature on policy iteration using the Euler equation includes Deaton (1991) and Li and Stachurski (2014).

is not chosen to maximize the Q function *at each* t , then FOCs remain only necessary conditions. The following section turns to understanding when and how the EGM is well-defined for step (A) above, and then turns to how to select the optimal roots in step (B).

4. MULTIDIMENSIONAL EGM WITH DISCRETE-CONTINUOUS CHOICES

This section formalizes EGM in the general setup outlined above. Section 4.1 starts by defining EGM formally as an inverse optimization problem on the space of exogenous ‘observed’ variables, which we define as the product space of post-states and constraint multipliers. We then turn to the second key contribution of our paper – the necessary and sufficient conditions for this inverse problem to be well-defined. In cases where an inverse does not exist on the full-dimensional exogenous sub-space of feasible observables, we also provide the conditions under which the exogenous grid can be defined as a subset of a lower-dimensional sub-manifold of the post-state space. We continue in Section 4.2 with the third key contribution of our paper – presenting the RFC algorithm that eliminates sub-optimal points in the presence of discrete choices. Importantly, we also provide error bounds for the EGM, which hold for the general case without discrete choices too. Throughout this section we will fix time t , the shock realization w_t , the discrete state z_t , and the discrete choice d_t as a tuple ξ_t .

4.1. EGM setup and invertibility.

4.1.1. *EGM setup.* EGM has been understood informally as a method to solve the policy function y_t by fixing y_t in an exogenous grid, and then finding values of the state m_t such that y_t satisfies the Euler equation. In contrast to the forward problem, this means the EGM is an inverse optimization problem, where one solves for *inputs* m_t given *observed outputs* y_t . However, recalling the Euler equation (EO2), when constraints bind, the value of the multiplier μ_t will also determine the current state in an inverse problem. Our innovation is to formalize the EGM as an inverse problem over the space of post-states and multipliers which contain the *observed information* we can use to determine the current state. In addition to the approach following naturally from recent advances in the theory of inverse problems (Iyengar and Kang, 2005), our method leads to significant computational advantages since it sharply identifies which constraint binds from information in the exogenous grid.²⁰

In terms of notation, we will use a_t , where $a_t = (y_{1,t}, \dots, y_{N_Y,t}, \mu_{1,t}, \dots, \mu_{N_g,t})$, to denote an end-of-period ‘observed’ variable. Letting $\Upsilon_t \subset \mathbb{R}_+^{N_g}$ be the range of the function μ_t , we will use $A_t = Y_t \times \Upsilon_t$ to denote the space of end-of-period observed variables. Finally, define a function mapping the active state to observables $\sigma_t: \bar{M}_t \rightarrow A_t$ such that $\sigma_t(\bar{m}_t) = (\bar{y}_t(\bar{m}_t), \bar{\mu}_t(\bar{m}_t))$. The term $\sigma_t^{\bar{d}_{t+1}}$ will refer to the function mapping the active state to the observed variables given feasible future discrete choices $[d_t, \bar{d}_{t+1}]$.²¹

²⁰Druehdahl and Jørgensen (2017) follows an approach where the inverse operator is defined over the product space of post-states and controls. In contrast, we define a formal inverse that maps directly to the FOCs of the S-function, and thus directly identifies where constraints bind. See Remark 2 below.

²¹Recall that d_t is fixed in this section.

Not all possible observed variables will satisfy the constraints and complementary slackness condition **(EO3)**. In particular, given ξ_t , let IB denote the set of all subsets of indices indexing the set of constraints defined on the active state space $\{\bar{g}_{1,t} \dots, \bar{g}_{N_g,t}\}$. Fixing $\text{IB}_l \in \text{IB}$, let \bar{g}_t^l denote the vector of binding constraint functions. Solutions will belong to different ‘constrained regions’ K_l associated with each subset $\text{IB}_l \in \text{IB}$ of binding constraints

$$(14) \quad K_{l,t} = \left\{ (\bar{m}_t, y_t) \in \text{Gr}\bar{\Gamma}_t, \mu_t \in \Upsilon_t \mid \bar{g}_t^l(\bar{m}_t, y_t) = 0, \mu_t \circ \bar{g}_t(\bar{m}_t, y_t) = 0 \right\}$$

Recalling the definition of the projection π_A , the space $K_{l,t}^A = \pi_A K_{l,t}$ denotes the possible observables within a constrained region that we could invert from, and $K_t^A = \bigcup_{l \in \text{IB}} \pi_A K_{l,t}$ becomes the space of all observables satisfying the constraints and complementary slackness conditions **(EO3)**.

Let us assume that the next period solution and the *function* Λ_{t+1} are known. Define the global EGM inverse problem²² as

$$(10) \quad \Theta_t(y_t, \mu_t) = \left\{ \bar{m}_t \in \bar{M}_t \mid \bar{\mathbf{E}}_{y,t}(y_t, \mu_t \mid \bar{m}_t) = 0, \right. \\ \left. \mathbf{d}_{t+1}(x_{t+1}) = \arg \max_{\vec{d}'} Q_t^{\vec{d}'}(\bar{x}_t, y_t, d_t) \right\}, \quad (y_t, \mu_t) \in K_t$$

where $x_{t+1} = (w_{t+1}, z_{t+1}, m_{t+1})$, $m_{t+1} = F_t^m(d_t, y_t, w_{t+1})$, \vec{d}' is feasible,²³ and the function \mathbf{d}_{t+1} maps the state variable x_{t+1} to future sequences of discrete choices. The definition incorporates Item (2). of Proposition 1 – i.e., finding a solution to the global inverse problem requires ensuring the future sequence of discrete choices implied by the post-state is optimal at time t . On the other hand, when we only compute roots to the Euler equations, we solve the following EGM inverse problem:

$$(10\text{-FOC}) \quad \Theta_t^F(y_t, \mu_t) = \left\{ \bar{m}_t \in \bar{M}_t \mid \bar{\mathbf{E}}_{y,t}(y_t, \mu_t \mid \bar{m}_t) = 0, \right. \\ \left. \mathbf{d}_{t+1}(x_{t+1}) = \arg \max_{\mathbf{d}} v_{t+1}^{\mathbf{d}}(x_{t+1}, w_{t+1}) \right\}, \quad (y_t, \mu_t) \in K_t$$

where $K_t = \bigcup_{l \in \text{IB}} K_{l,t}$. Computing $\Theta_t^F(y_t, \mu_t)$ becomes the task of the initial root-finding step in EGM (Step (A) in the computational procedure above). As mentioned, a solution to the inverse problem $\Theta_t^F(y_t, \mu_t)$ that uses only the FOCs may not mean that the implied sequence of future discrete choices $\mathbf{d}_{t+1}(x_{t+1})$ is optimal. One has to remove sub-optimal roots from $\Theta_t^F(y_t, \mu_t)$ to arrive at (the possible empty set) $\Theta_t(y_t, \mu_t)$ using Step (B) above.²⁴ It follows that the inverse problem Θ_t may not be defined everywhere on a region K_t^A since for given y_t , Item (2). of Proposition 1 may not hold.

4.1.2. Main results on invertibility. Before we turn to selecting the optimal roots (whether they be *analytical* or *numerical*) in $\Theta_t^F(y_t, \mu_t)$, a natural question that arises is whether or not Θ_t^F is

²²Without loss of generality, we have defined the EGM problem throughout this section on an active state space. When a strictly lower-dimensional active state space does not exist, the active state space can be trivially understood as the full current state space.

²³Through a slight abuse of notation, we have defined the Q function on the active state space.

²⁴However, when the necessary FOCs are inverted, the implied sequence of future discrete choices \vec{d}_{t+1} still maximizes the next period value function.

well-defined on neighbourhoods in K_t^A . Suppose we know that the Euler equation can be inverted at a point in K_t^A – i.e., that a solution exists for some future sequence of discrete choices. Does this mean we can construct an exogenous grid in a surrounding neighbourhood that is embedded in K_t^A ? It may be that an inverse of the Euler equation is not defined around a full-dimensional neighbourhood of a solution point (see Section 5.2). And moreover, what is the dimension and topological structure of $\sigma_t^{\vec{d}}(\bar{M}_t)$ compared to K_t ?

The first assumption we require for invertibility is a standard rank condition on the constraints, which guarantees the multipliers are unique. The second assumption we require for invertibility is continuity of the policy function given a future sequence of discrete choices.²⁵

Assumption (I.1) The cardinality of $\{i \mid \bar{g}_{i,t}(\bar{m}_t, y_t) = 0\}$ equals the rank of $\partial_y \bar{g}_t(m_t, y_t)$ for every $(\bar{m}_t, y_t) \in \text{Gr} \bar{\Gamma}_t$.

Assumption (I.2) For every feasible \vec{d}_{t+1} , the optimal policy function $\bar{y}_t^{\vec{d}_{t+1}}$ is continuous.

We start with a necessary condition, and focus on the unconstrained case for simplicity. Suppose we could construct an exogenous grid embedded in an open neighbourhood in Y_t and invert from it to a compact subset of the active state-space. This situation can be dubbed ‘pure EGM’ since we invert from a full-dimensional subset of the exogenous space. The necessary condition tells us that for the inverse problem (**IO-FOC**) to be well-defined, the dimension of the post-state space must equal the dimension of the active state space. The necessary condition also applies to the general case where the policy function may not be globally invertible but may be locally invertible.²⁶ For this result, consider the restriction of \bar{y}_t to a compact non-trivial interval $\bar{C} \subset \bar{M}_t$, denoted by $\bar{y}_t|_{\bar{C}}$.

Claim 1. *Let Assumption I.2 hold. If $\bar{y}_t|_{\bar{C}}$ is injective, $\bar{y}_t(\bar{C}) \subset \{y_t \mid \bar{g}_t(\xi_t, \bar{m}, y_t) > 0, \bar{m} \in \bar{M}\}^\circ$, and $\bar{y}_t|_{\bar{C}}^{-1}$ is well-defined on an open neighbourhood in Y_t° , then $N_{\bar{M}} = N_Y$.²⁷*

As for the sufficient conditions for invertibility of pure EGM, we can use Claim 1 to guide us: for pure EGM to be well-defined, the space we invert from must be a sub-manifold that is homeomorphic to \mathbb{R}^{N_M} . The inverse problem must then be defined on a manifold given by the graph of a continuous function of N_M ‘exogenous observables’ that then determines the current state.

To formalize the sufficient condition, we use \tilde{Y} and $\tilde{\Upsilon}$ to denote the \tilde{N}_Y , and \tilde{N}_g indices of exogenous post-states and exogenous multipliers, respectively. Moreover, let $\tilde{Y}_t = \times_{i \in \tilde{I}_Y} Y_{i,t}$, $\tilde{\Upsilon}_t = \times_{i \in \tilde{I}_\mu} \Upsilon_{i,t}$ and $\tilde{A}_t = \tilde{Y}_t \times \tilde{\Upsilon}_t$. For a given a_t , note that we can fix the multipliers taking

²⁵The continuity assumption is benign since given a future sequence of discrete choices, problem (**CS-DP**) can be solved as a standard concave dynamic programming problem, yielding continuous policies. Modern results characterize existence and continuity even in the absence of bounded rewards or compact feasibility correspondences (Feinberg et al., 2012).

²⁶For instance, potentially non-monotone, inverted U shaped policy functions.

²⁷Through a slight abuse of notation, the superscript \vec{d}_{t+1} is dropped in the Claim to save on notation. One can also view this result as the minimum requirement on dimensionality for pure EGM to be well-defined, even in the absence of discrete choices.

on values in $\Upsilon_t \setminus \tilde{\Upsilon}_t$ along $N_g - \tilde{N}_g$ indices, and the non-exogenous post-states taking on values in $Y_t \setminus \tilde{Y}_t$ along $N_Y - \tilde{N}_Y$ indices. We can then map the exogenous variables back to A_t using an embedding $\text{em}_{\tilde{A}}: \tilde{A}_t \rightarrow A_t$. Next, we can also select elements from the vector $\bar{\mathbf{E}}_{a,t} = [\bar{\mathbf{E}}_{y,t}, \bar{\mathbf{E}}_{\mu,t}]$ along the N_Y indices of (i) multipliers associated with the binding constraints, and (ii) indices of post-states i such that $\partial_{y_i} \bar{g}_t^l(\bar{m}_t, y_t) = 0$, to define a projection $\pi_{N_Y}: \mathbb{R}^{N_Y + N_g} \rightarrow \mathbb{R}^{N_Y}$.²⁸

Theorem 2. (Invertibility of pure EGM) Fix $\text{IB}_l \in \text{IB}$. If $\tilde{N}_Y + \tilde{N}_g = N_Y = N_M$ and there exists

- (1) $\bar{m}_t \in M_t^\circ$ and $(y_t, \mu_t) \in (K_{l,t}^A)^\circ$ such that $y_t = \bar{y}_t^{\bar{\mathbf{d}}_{t+1}}(\bar{m}_t)$ for feasible $\bar{\mathbf{d}}_{t+1}$, and
- (2) given (y_t, μ_t) , an embedding $\text{em}_{\tilde{A}}: \tilde{A}_t \rightarrow A_t$ and projection $\pi_{N_Y}: \mathbb{R}^{N_Y + N_g} \rightarrow \mathbb{R}^{N_Y}$ such that
- $$(15) \quad \det \partial_{\bar{m}} \pi_{N_Y} \bar{\mathbf{E}}_{a,t}(\bar{m}, \text{em}_{\tilde{A}}(\tilde{a})) \neq 0$$
- for all $(\text{em}_{\tilde{A}}(\tilde{a}), \bar{m}) \in K_{l,t}$ with $\tilde{a} \in (\pi_{\tilde{A}} K_{l,t})^\circ$,

then there exists a continuous function φ and neighbourhood $U \subset \tilde{A}_t$ of $(\tilde{y}_t, \tilde{\mu}_t)$, such that for any $\tilde{e} \in U \subset (\pi_{\tilde{A}} K_{l,t})^\circ$, $\Theta_t^F(\varphi(\tilde{e}))$ is non-empty. Moreover, if $\bar{m} \in \Theta_t^F(\varphi(\tilde{e}))$ then $(\bar{m}, \varphi(\tilde{e})) \in K_{l,t}$.

Suppose we know a solution (\bar{m}_t, y_t, μ_t) exists in the interior of $K_{l,t}$. To check the conditions for Theorem 2, we must select \tilde{N}_g multipliers and \tilde{N}_Y exogenous post-states such that

- (A) $\tilde{N}_g + \tilde{N}_Y = N_Y = N_M$,
- (B) the vector $\pi_{N_Y} \bar{\mathbf{E}}_{a,t}(\bar{m}, \text{em}_{\tilde{A}}(\tilde{a}))$ consists of (i) multipliers associated with the binding constraints, and (ii) indices of post-states i such that $\partial_{y_i} \bar{g}_t^l(\bar{m}_t, y_t) = 0$,²⁹ and
- (C) the determinant of $\partial_{\bar{m}} \pi_{N_Y} \bar{\mathbf{E}}_{a,t}(\bar{m}, \text{em}_{\tilde{A}}(\tilde{a}))$ is non-zero - i.e., (15) holds - for every \tilde{a} in the interior of the constrained region along the exogenous variables, $\pi_{\tilde{A}} K_{l,t}$.

Under these conditions, we can construct an exogenous grid in the interior of $\pi_{\tilde{A}} K_{l,t}$, and for \tilde{a} in the grid, we are guaranteed to find \bar{m} satisfying $\pi_{N_Y} \nabla_a \bar{\mathbf{S}}_t(\bar{m}, \text{em}_{K^A}(\tilde{a}) | \bar{m}, \bar{\Xi}_t) = 0$ (recall we have fixed Λ_{t+1}). For a permutation ν , the optimal policy given some $\bar{\mathbf{d}}_{t+1}$ and \bar{m} will then be defined by $y = (y_{\nu_1}, \dots, y_{\nu_{\tilde{N}_Y}}, y_{\nu_{\tilde{N}_Y+1}, t}, \dots, y_{\nu_{N_Y}, t})$, where $y = \pi_Y \text{em}_{\tilde{A}} \tilde{a}$.³⁰ Under Assumption I.1, we can then recover the complete set of multipliers by solving for μ using $\mu \mapsto \nabla_a \bar{\mathbf{S}}_t(\bar{m}, y, \mu | \bar{m}, \bar{\Xi}_t) = 0$.

Importantly, if we define the exogenous grid to be a subset of $K_{l,t}^A$, since $K_{l,t}^A$ incorporates the complementary slackness conditions, we can recover *information about the optimally binding constraints*. The inverse obtained by the EGM will thus furnish a state \bar{m} such that the optimal

²⁸Under Assumption I.1, the number of multipliers associated with the binding constraints is equal to the number of post-states such that $\partial_{y_i} \bar{g}_t^l(\bar{m}_t, y_t) \neq 0$. As such, the sum of post-states such that $\partial_{y_i} \bar{g}_t^l(\bar{m}_t, y_t) = 0$ and multipliers associated with the binding constraints is equal to N_Y .

²⁹Note that $\tilde{a}_t = \pi_{\tilde{A}} a_t$ and for a_t , we have $a_t = \text{em}_{\tilde{A}} \tilde{a}_t$, where $a_t = (y_t, \mu_t)$.

³⁰The variables $y_{\nu_1}, \dots, y_{\nu_{\tilde{N}_Y}}$ in the vector y are the exogenous post-states, while the remaining variables are the post-states we held fixed to their value in y_t .

solution given \bar{m} and some \mathbf{d}_{t+1} is in the region $K_{l,t}^A$. During computation, this avoids any costly secondary upper envelope loops to choose the optimal constraint.³¹

Remark 2. Fix $\text{IB}_l \in \text{IB}$. Suppose \tilde{a}_t is a point in the exogenous grid, and we find \bar{m}_t such that $\bar{m}_t \in \Theta_t^F(\varphi(\tilde{a}_t))$ by applying the EGM. By Proposition 1, the observable a_t , with $a_t = \varphi(\tilde{a}_t)$, solves (CS-DP) given \bar{m}_t .

So far, we assumed that within a constrained region $K_{l,t}$, a solution point exists and we studied the dimension and structure of an exogenous grid surrounding this point. Verifying the second order condition (15) and delineating the exogenous observables seems to be a minimum requirement before computing any practical high-dimensional model. A stronger result, guaranteeing that an inverse exists everywhere in the region of constrained observables, can be obtained by checking the conditions of the well-known Poincaré-Miranda Theorem.

Corollary 2. Consider the setting of Theorem 2. If for each $a \in \pi_A K_{l,t}$, there exists $I = \times_{i=1}^{N_M} [\hat{m}_{i,t}^{\min}, \hat{m}_{i,t}^{\max}] \subset \bar{M}_t$ and $(\iota_1, \dots, \iota_{N_M}) \in \{-1, 1\}^{N_M}$ such that for each $j \in \{1, \dots, N_M\}$ and every $\bar{m}_{k,t} \in [\hat{m}_{k,t}^{\min}, \hat{m}_{k,t}^{\max}]$ with $k \neq j$, we have

$$(16) \quad \iota_j \bar{\mathbf{E}}_{a,t}(\bar{m}_1, \dots, \bar{m}_{j-1}, \dots, \hat{m}_j^{\min}, \bar{m}_{j+1}, \dots, \bar{m}_{N_M}, \text{em}_{\bar{A}}(\tilde{a})) \leq \iota_j \bar{\mathbf{E}}_{a,t}(\bar{m}_1, \dots, \bar{m}_{j-1}, \dots, \hat{m}_j^{\max}, \bar{m}_{j+1}, \dots, \bar{m}_{N_M}, \text{em}_{\bar{A}}(\tilde{a}))$$

then for each $a \in \pi_A K_{l,t}$, $\Theta_t^F(a)$ is well-defined. Moreover, if the conditions of Theorem 2 hold, then given feasible $\vec{\mathbf{d}}_{t+1}$, there exists a continuous inverse $\vec{\mathbf{a}}_t^{\vec{\mathbf{d}}_{t+1}, -1}$ defined on $\pi_A K_{l,t}$ such that $\vec{\mathbf{a}}_t^{\vec{\mathbf{d}}_{t+1}, -1}(a) = \Theta_t^F(a)$.

By examining (EO2) we see that verifying the conditions of the Poincaré-Miranda Theorem and (15) above is straightforward, as it only involves knowing how the primitive functions (i.e., the reward and constraint functions) behave as an argument of the state (see Section 5.1). The intuition for the proof (which we provide in the online appendix) of why this is true mirrors the deeper EGM intuition in Carroll (2006); the invertibility of the policy function and the convex constraint choice depends only on the mapping of information from the post-state to the state that, given the shadow value, is defined by the primitive functions.

Let us now address the case where the dimension of the active state space is strictly lower than the post-state space. Pure EGM will not be well-defined. However, suppose the policy functions and multipliers are locally injective. So if we were to invert back from an exogenous grid, what would the structure of the exogenous grid be?

Assumption (I.3) For a compact set $\bar{C} \subset M_t$, and for each feasible $\vec{\mathbf{d}}_{t+1}$, the restriction of $\sigma_t^{\vec{\mathbf{d}}_{t+1}}$ to \bar{C} is locally injective and continuous onto its own image.

³¹In contrast, Druedahl and Jørgensen (2017) applies the EGM over constrained regions that are not defined by the complementary slackness conditions.

Claim 2. *If Assumption I.3 holds, then for each feasible \vec{d}_{t+1} , $\dim(\sigma_t^{\vec{d}_{t+1}}(\bar{C})) = N_{\bar{M}}$.*

This claim answers our question by telling us that the dimension of the exogenous grid (which must be a subset of the image of the functions $\sigma_t^{\vec{d}_{t+1}}$) must be the same as the dimension of the active state space, and even when none of the constraints bind, the image of the policy functions will be a lower-dimensional sub-manifold of the post-state space. Since $\sigma_t^{\vec{d}_{t+1}}$ is an embedding, an implication is that a $N_{\bar{A}}$ -dimensional sub-manifold of A_t can be constructed by a map from $\mathbb{R}^{N_{\bar{A}}}$ to $\mathbb{R}^{N_g + N_Y - N_{\bar{A}}}$ defined by the mapping of the post-state to the shadow value $y \mapsto \mathbb{E}_{x_t} \Lambda_{t+1} \partial_y F_t^m(w_{t+1}, y)$ (see Section 5.2).

Corollary 3. *If Assumption I.3 holds, then $\sigma_t(\bar{C})$ is an $N_{\bar{A}}$ -dimensional sub-manifold of A_t . Moreover, if $N_{\bar{A}} < N_g + N_Y$, then for each $y, \mu \in \sigma_t(\bar{C})$, there exists an open set $O \subset \mathbb{R}^{N_{\bar{A}}}$, an open set $U \subset \mathbb{R}^{N_g + N_Y}$ with $y, \mu \in U$, and a mapping $\text{sm}: \mathbb{R}^{N_{\bar{A}}} \rightarrow \mathbb{R}^{N_g + N_Y - N_{\bar{A}}}$ such that*

$$\begin{aligned} Y_t \times \Upsilon_t \cap U &= \left\{ y, \mu \mid \left(y_{\iota_y(n_1+1)}, \dots, y_{\iota_y(N_Y)}, \mu_{\iota_\mu(n_2+1)}, \dots, \mu_{\iota_\mu(n_{N_g})} \right) \right. \\ &\quad \left. = \text{sm} \left(y_{\iota_y(1)}, \dots, y_{\iota_y(n_1)}, \mu_{\iota_\mu(1)}, \dots, \mu_{\iota_\mu(n_2)} \right) \right\}, \quad n_1 + n_2 = N_{\bar{A}} \end{aligned}$$

where ι_μ and ι_y are permutations of the indices of the multipliers and post-states, respectively.

4.1.3. *EGM grids in practice.* To computationally implement EGM, we define it as a tuple

$$\left(\Theta_t^F, K_t, (\mathcal{A}_{l,t})_{l \in \text{IB}}, \{\kappa_t^{\vec{d}_{t+1}}\}_{\vec{d}_{t+1}} \right)$$

The set of grid points $\mathcal{A}_{l,t}$ denotes the exogenous grid, which must satisfy

$$(17) \quad \mathcal{A}_{l,t} \subset \bigcup_{\vec{d}_{t+1}} \sigma_t^{\vec{d}_{t+1}}(\bar{M}_t) \cap K_{l,t}$$

where the union is taken over all future discrete choices such that $[d_t, \vec{d}_{t+1}]$ is feasible given some $\bar{m}_t \in \bar{M}_t$. The term $\sigma_t^{\vec{d}_{t+1}}(\bar{M}_t)$ is the image of the active state space under the observable function. For each l , $\mathcal{A}_{l,t}$ is a finite subset of an $N_{\bar{M}}$ -dimensional space embedded in A_t . The set $\{\kappa_t^{\vec{d}_{t+1}}\}_{\vec{d}_{t+1}}$ contains ‘grid distance functions’ where $\kappa_t^{\vec{d}_{t+1}}: \sigma_t^{\vec{d}_{t+1}}(\bar{M}_t) \rightarrow \mathbb{R}^{N_{\bar{M}}}$ for each feasible \vec{d}_{t+1} . While we do not need to explicitly evaluate the functions $\kappa_t^{\vec{d}_{t+1}}$ for each \vec{d}_{t+1} , placing restrictions on their curvature will be used to implement the RFC algorithm and plays a key role in guaranteeing convergence of the EGM solution and its asymptotic error bound. In practice, we will need to be able to evaluate a function κ_t , with $\kappa_t(a_t)$ denoting the evaluation $a_t \mapsto \kappa_t^{\mathbf{d}_{t+1}(a_t)}(a_t)$, where $\mathbf{d}_{t+1}(a_t)$ is the optimal future sequence of discrete choices implied in $t+1$ by the observable a_t . We discuss these distance functions in greater detail below and in the applications.

Elements of \mathcal{A}_t will be denoted $a_{t,i}^\#$ and depending on the context, we use $a_{t,i}^\#$ and $(y_{t,i}^\#, \mu_{t,i}^\#)$ interchangeably. The EGM fixes - or ‘observes’ - a finite sequence (i.e., exogenous grid), and the objective is to obtain the corresponding endogenous grid $\mathcal{M}_t^* \subset M_t$ by solving the inverse problem **(IO)** such that

$$(18) \quad m_{t,i}^\# \in \Theta_t(y_{t,i}^\#, \mu_{t,i}^\#), \quad \forall y_{t,i}^\#, \mu_{t,i}^\# \in \mathcal{A}_t, m_{t,i}^\# \in \mathcal{M}_t$$

Next, let $x_{t,i}^\# = (w_t, m_{t,i}^\#, z_t)$ and let I^A be the index set for the exogenous grid. Further grids are set as below:

- (1) The grid of ‘objective values’ $\mathcal{V}_t^\star = \left\{ Q_t(x_{t,i}^\#, y_{t,i}^\#, d_{t,i}) \right\}_{i \in I^A}$ obtained by evaluating (\mathbf{Q}) .
- (2) The subset of the exogenous grid points that are optimal given their associated endogenous grid point $\mathcal{A}_t^\star = \left\{ y_{t,i}^\#, \mu_{t,i}^\# \in \mathcal{A}_t \mid \Theta_t(y_{t,i}^\#, \mu_{t,i}^\#) \neq \emptyset \right\}$.

The endogenous grid generated by the necessary conditions (**IO-FOC**) will be denoted by \mathcal{M}_t^F , with $\mathcal{M}_t^F \subset \bar{\mathcal{M}}_t$, satisfying

$$m_{t,i}^\# \in \Theta_t^F(y_{t,i}^\#, \mu_{t,i}^\#), \quad \forall y_{t,i}^\#, \mu_{t,i}^\# \in \mathcal{A}_t, m_{t,i}^\# \in \mathcal{M}_t^F$$

As such, define

- (3) The grid of objective values of the future choice-specific value functions $\mathcal{V}_t^F = \left\{ Q_t(x_{t,i}^\#, d_t, y_{t,i}^\#) \right\}_{i \in I^A}$ obtained by evaluating (\mathbf{Q}) .³²
- (4) The grid of sup-gradients of the future discrete choice-specific value functions \mathcal{V}_t^F with respect to the state as $\nabla \mathcal{V}_t^F$ (recall Corollary 1 and evaluate the sup-gradients using (\mathbf{L}) at the exogenous and endogenous grid points).

Remark 3. It follows from Item (1). of Proposition 1 that any element $v_{t,i}^\# \in \mathcal{V}_t^F$ will correspond to a future sequence of discrete choices $\mathbf{d}_{t+1}(x'_{t+1,i})$ that are optimal at time $t+1$. In particular, $v_{t,i}^\# = u_t(x_{t,i}^\#, d_t, y_{t,i}^\#) + \mathbb{E}_{x_t^\#} v_{t+1}^{\bar{\mathbf{d}}_{t+1}}(x'_{t+1,i}) = v_t^{\bar{\mathbf{d}}_t}(x_{t,i}^\#)$, where $\bar{\mathbf{d}}_t = [d_t, \mathbf{d}_{t+1}(y_{t+1,i}^\#)]$, $x_{t,i}^\# = (w_t, z_t, m_{t,i}^\#)$ and $x'_{t+1,i} = F_t(d_t, y_{t,i}^\#, w_{t+1})$.

Remark 4. Since the FOCs are necessary, $\mathcal{M}_t^\star \subset \mathcal{M}_t^F$, where the inclusion may be strict.

4.2. Rooftop-cut algorithm. When $\mathcal{M}_t^\star \subset \mathcal{M}_t^F$ is a proper subset, the task is to remove sub-optimal points in the endogenous grid \mathcal{M}_t^F , and produce a set as close as possible to \mathcal{M}_t^\star . To do so, we propose the RFC algorithm.

Recall from our discussion below (**BE-2**) and Remark 3 that each exogenous grid point $a_{t,i}^\#$ implies a particular future stochastic sequence of discrete choices \mathbf{d}_{t+1} . We do not know, however, if this future sequence is optimal given the current state implied by the endogenous grid point $m_{t,i}^\#$. The RFC algorithm uses the *sup-gradients of the future choice-specific value functions* (recall Figure 1) in the $\nabla \mathcal{V}_t^F$ grid to determine if neighbouring points in the endogenous grid are optimal or sub-optimal. To implement the algorithm in practice, we first set a ‘jump detection threshold’ $\bar{J} > 0$ and a ‘search radius’ $\rho_r > 0$. Let I^F denote the index set of the points in \mathcal{M}_t^F , and initialize $I^{\text{cut}} \equiv \{\}$. The RFC algorithm proceeds as follows:

³²Recall from Section 2.3.1 that objective values may be sub-optimal at time t .

Box 1: RFC algorithm

For each $j \in I^F$,

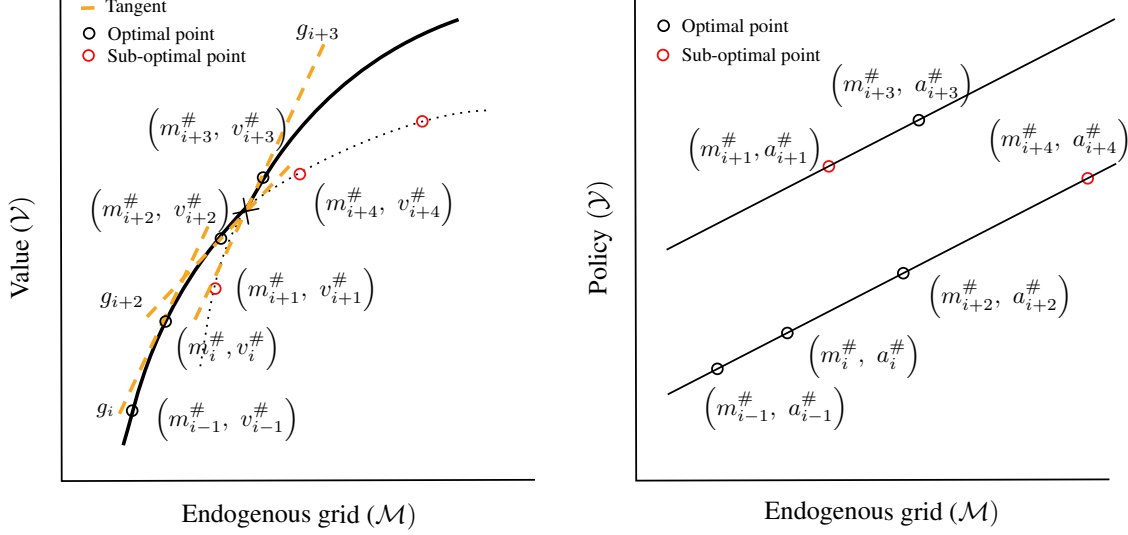
- (1) Construct a tangent plane to the future choice specific value function at $m_{t,j}^\#$ using the sup-gradient $\nabla v_{t,j}^\# \in \nabla \mathcal{V}_t^F$ at the value $v_{t,j}^\# \in \mathcal{V}_t^F$. The tangent plane is given by $m^\# \mapsto \nabla v_{t,j}^\# \circ (m^\# - m_{t,j}^\#)$.
- (2) For each l such that $m_{t,l}^\# \in \mathbb{B}_{\rho_r}(m_{t,j}^\#) \cap \mathcal{M}_t^F$,
 - (i) if the tangent plane $m^\# \mapsto \nabla v_{t,j}^\#(m^\# - m_{t,j}^\#)$ dominates the value $v_{t,l}^\#$ at the endogenous grid point $m_{t,l}^\#$ – i.e., $\nabla v_{t,j}^\# \circ (m_{t,l}^\# - m_{t,j}^\#) > v_{t,l}^\#$, and
 - (ii) if the relative difference between the exogenous grid points at j and l in the distance κ_t is greater than \bar{J} – i.e., $\frac{\kappa_t(a_{t,j}^\# - a_{t,l}^\#)}{\|m^\# - m_{t,j}^\#\|} > \bar{J}$,
 then append l to I^{cut} .

Once the steps above are completed for each $j \in I^F$, the optimal grid points are recovered by deleting the dominated neighbouring points from the endogenous grid, thus constructing an index set $I^{\text{RFC}} := I \setminus I^{\text{cut}}$. The grids constructed by the RFC algorithm will be

$$(19) \quad \mathcal{M}_t^{\text{RFC}} = \{m_{t,i}^\#\}_{i \in I^{\text{RFC}}}, \mathcal{A}_t^{\text{RFC}} = \{a_{t,i}^\#\}_{i \in I^{\text{RFC}}}, \mathcal{V}_t^{\text{RFC}} = \{v_{t,i}^\#\}_{i \in I^{\text{RFC}}}$$

To intuitively understand the algorithm, consider Figure 2 that demonstrates the RFC algorithm for a stylized one-dimensional problem. To simplify exposition, assume κ is the identity function and assume we are considering an unconstrained problem. Both panels show the endogenous grid points in \mathcal{M}_t^F on the x-axis. On the y-axis, the left panel shows the points of the future choice-specific values in \mathcal{V}_t^F , while the right panel shows the policy function values in the grid \mathcal{V}_t^F . The points $(m_{t,i-1}^\#, v_{t,i-1}^\#)$, $(m_{t,i}^\#, v_{t,i}^\#)$, $(m_{t,i+2}^\#, v_{t,i+2}^\#)$, and $(m_{t,i+3}^\#, v_{t,i+3}^\#)$ are on the upper envelope, while the points $(m_{t,i-1}^\#, a_{t,i-1}^\#)$, $(m_{t,i}^\#, a_{t,i}^\#)$, $(m_{t,i+2}^\#, a_{t,i+2}^\#)$, and $(m_{t,i+3}^\#, a_{t,i+3}^\#)$ define the optimal policy. In contrast, the point $(m_{t,i+1}^\#, v_{t,i+1}^\#)$ is not on the upper envelope, and the policy $(m_{t,i+1}^\#, a_{t,i+1}^\#)$ is not optimal. Here note that the point $(m_{t,i+1}^\#, a_{t,i+1}^\#)$ ‘jumps’ from the point $(m_{t,i}^\#, a_{t,i}^\#)$ (see the right panel) since it is associated with a different future sequence of discrete choices. The point $(m_{t,i+1}^\#, a_{t,i+1}^\#)$ it is also dominated by the tangent to the future choice-specific value function at $(m_{t,i}^\#, v_{t,i}^\#)$ (see the left panel), and is thus removed. In contrast, while the point $(m_{t,i+3}^\#, a_{t,i+3}^\#)$ also ‘jumps’ from the point $(m_{t,i}^\#, a_{t,i}^\#)$, this point dominates the tangent, and is thus retained. The point $(m_{t,i+4}^\#, a_{t,i+4}^\#)$ is similarly removed.

How do we choose the functions $\kappa^{\mathbf{d}_{t+1}}$, the jump detection threshold \bar{J} , and the search radius ρ_r ? We briefly describe the practical considerations here and turn to a formal analysis in the next section. For each feasible future sequence of discrete choices \mathbf{d}_{t+1} , we require $\kappa^{\mathbf{d}_{t+1}}$ to be a function such that the function $\hat{\kappa}^{\mathbf{d}_{t+1}}$ defined by $\bar{m} \mapsto \kappa^{\mathbf{d}_{t+1}}(\sigma_t^{\mathbf{d}_{t+1}}(\bar{m}))$ is Lipschitz with constant no greater than L_1 , and has a Lipschitz inverse with constant no greater than L_2 . This allows us to relate the exogenous grid spacing to the endogenous grid spacing. In many applications, the function

**Figure 2.** The RFC algorithm

mapping the state to ‘controls’ such as the consumption function can serve as $\kappa^{d_{t+1}}$. The function κ_t simply becomes the control choice implied by an observable in the exogenous grid.³³

The choice of the jump detection threshold can be made based on the maximum possible curvature of the functions $\kappa^{d_{t+1}}$ given a future sequence of discrete choices d_{t+1} . For instance, in a standard income fluctuation problem, the marginal propensities to consume are bounded above by one and bounded below by a constant that can be derived analytically (Carroll and Shanker, 2024), allowing us to set $\bar{J} \geq 1$. The search radius, on the other hand, can be chosen to be greater than the maximum ‘spacing between neighbouring points’ in the endogenous grid. Consider constructing an exogenous grid such that for a particular grid size, $|\mathcal{A}_t|$, there exists ϵ with $\|\kappa^{d_{t+1}}(a_{t,i}^\#) - \kappa^{d_{t+1}}(a_{t,j}^\#)\| < \epsilon$ for neighbouring exogenous points; then the search radius can be set to $\rho_r = 2\epsilon L_2$ since the maximum possible distance between the associated endogenous grid points will be ϵL_2 (see Remark 6).

Finally, depending on the particular application, it may be more practicable to apply RFC iteratively or sequentially via search or scan methods to reduce the need to compute all pair-wise tangent conditions. We discuss these practical implications in Section 5.

4.2.1. Intersection points. We can also use the first order information in the RFC algorithm to easily add an approximation of the intersection points of two different future choice-specific value functions. In Figure 2, the point \times is an approximation of the intersection of the future choice-specific value functions. When a neighbouring point l lies above a tangent plane to the future choice-specific value function at j , the intersection point can be found by finding the intersection of the two lines $p \mapsto (m_{t,j}^\#, v_{t,j}^\#) + p \circ \nabla v_{t,j}^\#(m_{t,l}^\# - m_{t,j}^\#)$ and $p \mapsto (m_{t,l}^\#, v_{t,l}^\#) + p \circ \nabla v_{t,l}^\#(m_{t,j}^\# - m_{t,l}^\#)$.

³³For instance, consider a standard income fluctuation problem (Li and Stachurski, 2014) with an artificial liquidity constraint and i.i.d shocks. For the constrained region, we can set $\kappa(\mu_t, y_0) = \partial u^{-1}(\mu_t)$, where ∂u^{-1} is the inverse of the marginal utility and μ_t is a value of the multiplier associated with the liquidity constraint. For unconstrained region, $\kappa(0, y_t) = \partial u^{-1}(\mathbb{E}\Lambda_{t+1}(y_t))$.

We can also add the optimal policy at the intersection points. In particular, suppose $m_{t,\times}^\#$ is an approximated intersection point between $m_{t,l}^\#$ and $m_{t,j}^\#$. We can perform a nearest neighbour search around the point $m_{t,j}^\#$ in the original grid \mathcal{A}_t and find neighbouring points $\{m_{t,i}^\#, y_{t,i}^\#\}_i$ such that the observable values do not ‘jump’ from the point j . An interpolant can be constructed using these neighbouring points to locally approximate the optimal policy given the optimal future discrete choice implied by $m_{t,j}^\#$. This interpolant can be evaluated at $m_{t,\times}^\#$ to produce an approximate policy $y_{t,\times}^\#$. To ensure jumps in the policy are approximated, an approximate policy interpolated using neighbours to the policy at $m_{t,l}^\#$ can also be attached at an arbitrarily small distance from $m_{t,\times}^\#$. We note that in applications with many states, it may be more practicable to approximate policies at the intersection by nearest neighbour interpolation, a procedure that performs well in the first application we study below - see Section 5.1.2).

4.2.2. Vectorization. A key advantage of the RFC algorithm is that it can be made highly efficient using vectorized computation (Harris et al., 2020), making it possible for high-dimensional discrete-continuous applications to exploit the massive parallelism offered by GPUs. In particular, the deviation in the objective values between a point and its other neighbouring points can be represented by $(\mathcal{V}_t - \mathcal{V}_t^{\text{neigh}})$, where $\mathcal{V}_t^{\text{neigh}}$ is a matrix such that each j ’th row is a list of the objective values of the ι -neighbouring points to j . Similarly, $|(\mathcal{Y}_t - \mathcal{Y}_t^{\text{neigh}})/(\mathcal{M}_t - \mathcal{M}_t^{\text{neigh}})|$ becomes a matrix of gradients of each policy value to neighbouring policy values. We can then compute the sub-optimal points via the Boolean operation

$$(20) \quad I^{\text{cut}} = \left((\mathcal{M}_t - \mathcal{M}^{\text{neigh}_t}) \otimes \nabla \mathcal{V}_t > (\mathcal{V}_t - \mathcal{V}^{\text{neigh}_t}) \right) \circ \left(|\mathcal{Y}_t - \mathcal{Y}^{\text{neigh}_t}| / \|(\mathcal{M}_t - \mathcal{M}^{\text{neigh}_t})\| > \bar{J} \right),$$

where \otimes is the tensor dot product defined over the appropriate axes. The result I^{cut} is a tensor whose i, j ’th entry determines whether grid point j is sub-optimal. Since this equation represents the RFC algorithm using tensor algebra, the algorithm can be easily programmed without ‘loops’ to exploit array programming packages such as NUMPY, GOOGLE JAX and CUDA.³⁴

4.2.3. Convergence and error bound. In this subsection, Theorem 2 or Claim 2 conditions will be in force. We now state the assumptions used for our theoretical results on the RFC algorithm.

The first assumption states that we formally study the exogenous grid as a simplicial complex generated by the image of the grid distance functions.

Assumption (E.1) For each feasible \vec{d}_{t+1} , the points $\kappa_t(\sigma_t^{\vec{d}_{t+1}}(\bar{M}_t) \cap \mathcal{A}_t)$ generate a simplicial complex $\mathbb{K}^{\vec{d}_{t+1}}$.

The second assumption requires that we can control the grid spacing of the exogenous grid using the functions $\kappa_t^{\vec{d}_{t+1}}$. Let $|\mathcal{A}_t|$ denote the number of exogenous grid points, and let $\epsilon_{|\mathcal{A}_t|}$ denote the maximum circumcircle of the simplices in $\cup_{\vec{d}_{t+1}} \mathbb{K}^{\vec{d}_{t+1}}$.

³⁴See Sargent and Stachurski (2024).

Assumption (E.2) $\lim_{|\mathcal{A}_t| \rightarrow \infty} \epsilon_{|\mathcal{A}_t|} = 0.$

The third assumption requires that the post-state policy functions (conditional on a future sequence of discrete choices) do not ‘change’ arbitrarily fast and works to bound the distance between endogenous grid points. The assumption is straightforward to verify in economic applications since quantities like marginal propensities to save and consume are bounded (see Section 5). Recall the definition of $\dot{\kappa}^{d_{t+1}}$ above.

Assumption (E.3) The family of functions $\{\dot{\kappa}^{d_{t+1}}\}_{d_{t+1}}$ are monotone and bi-Lipshitz with the Lipshitz constant $\dot{\kappa}^{d_{t+1}}$ no greater than L_1 , and the Lipshitz constant $\dot{\kappa}^{d_{t+1}, -1}$ no greater than L_2 .³⁵

For a function f , let us define $f \circ \sigma_t^{\text{INT}}$ to be the linear interpolant of the function $f \circ \sigma_t$ constructed using Barycentric coordinates of simplices in the Delauny triangulation of $\mathcal{M}_t^{\text{RFC}}$ and the points $f(\mathcal{A}^{\text{RFC}})$.

Theorem 3. (Asymptotic error bound) *Let Assumptions E.1 - E.3 hold and assume $L_2\epsilon < \rho_r$. If for each feasible d_{t+1} , $f \circ \sigma_t^{d_{t+1}}$ is Lipshitz with constant no greater than L_0 , then for any $\bar{m}_t \in \bar{M}_t$ such that $\sigma_t(\bar{m}_t) \in K_{t,l}^o$, there exists $\bar{\epsilon}$ such that for all $\epsilon < \bar{\epsilon}$, $\|f \circ \sigma^{\text{INT}}(\bar{m}_t) - f \circ \sigma(\bar{m}_t)\| < 3L_0L_2\epsilon$.*

While this is a worse case point-wise result, note we do not require assumptions on the number or type of jump discontinuities or monotonicity of the policy function. Furthermore, for applications, we are typically interested in the asymptotic accuracy of the moment conditions generated by the integrating policy function. The above result implies that if the functions $f \circ \sigma_t$ are bounded, then moment conditions will converge as the exogenous grid size increases.

Corollary 4. *Let Assumption 1 hold. If $\left[f \circ \sigma(\bar{m}_t^{\vec{d}_{t+1}})\right]^p$ is uniformly bounded and measurable for all feasible \vec{d}_{t+1} , then for $p \geq 1$, $\mathbb{E} \left[f \circ \sigma^{\text{INT}}(\bar{m}_t)\right]^p \rightarrow \mathbb{E} \left[f \circ \sigma(\bar{m}_t)\right]^p$ as $|\mathcal{A}_t| \rightarrow \infty$.*

The uniform boundedness condition is straightforward to satisfy if, for instance, the policy functions are bounded.

Remark 5. *Including the points of intersection between future choice-specific value functions does not affect the error bounds, since the intersection points are also a first order approximation. Moreover, the methods that include the intersection points - such as those proposed by Iskhakov et al. (2017) - will at best be subject to the error bound above since they rely on constructing secants between overlapping future choice-specific value functions.*

Remark 6. *Theorem 3 guides us on the size of the search radius. In particular, the search radius can be set to $2L_2\epsilon$. Thus, the search radius becomes twice the grid spacing on the exogenous grid, and is scaled by the maximum amount the EGM can ‘stretch’ distances on the endogenous grid L_2 .*

³⁵The family of d_{t+1} are all future discrete choices such that $[d_t, d_{t+1}]$ is feasible given some $\bar{m}_t \in \bar{M}_t$.

This ensures that each point in the endogenous grid is within a distance of the optimal point so that it can be ‘checked’ by the RFC algorithm.

5. APPLICATIONS

This section illustrates our theoretical results and the RFC algorithm using two well-known dynamic optimization applications related to (i) pension savings and retirement choice with unemployment risk, and (ii) housing investments with adjustment frictions. The online appendix and the public software repository additionally include two other applications for the RFC method – i.e., the models in Iskhakov et al. (2017) and Fella (2014), to illustrate the wide applicability of our method.

5.1. Application 1: Retirement and pension savings. Our first application uses the model by Druedahl and Jørgensen (2017) as a benchmark. In this context, let T be finite and consider the problem of an agent who chooses a post-state $y_t = (y_{f,t}, y_{p,t})$ that consists of end-of-period liquid (financial) assets $y_{f,t}$ and pension assets $y_{p,t}$ to maximize lifetime utility. The continuous state variables of the problem are start-of-period financial assets $m_{f,t}$ and pension assets $m_{p,t}$. Thus, the continuous state space is $M_t = M_{f,t} \times M_{p,t} = \mathbb{R}_+^2$ and the post-state space is $Y_t = Y_{f,t} \times Y_{p,t} = \mathbb{R}_+^2$. Each period, the agent can choose whether or not to work next period, with $d_t = 1$ denoting employment and $d_t = 0$ denoting retirement. The discrete state variable z_t captures the agent’s employment status at the beginning of the period. Accordingly, the discrete choice space and discrete state space are $D_t = \{0, 1\}$ and $Z_t = \{0, 1\}$, respectively.

Turning to the transition functions, we note that liquid assets evolve according to

$$(21) \quad m_{f,t+1} = (1 + r_f)y_{f,t} + z_{t+1}w_{t+1} + (1 - z_{t+1})(\bar{w} + (1 + r_p)y_{p,t})$$

where \bar{w} is the unemployment benefit paid to retirees. The rate of return on liquid assets is r_f , and the rate of return on pension assets is r_p . If an agent is employed at the beginning of a period, they receive a stochastic wage w_t , with w_t being log-normally distributed. If, however, the agent retires, they receive their pension balance as a lump-sum payment. The transition function for pension assets is then given by

$$(22) \quad m_{p,t+1} = z_{t+1}(1 + r_p)y_{p,t}$$

where pension assets only accumulate for workers. Each period that the agent works ($z_t = 1$), they can make a pension contribution $c_{p,t}$ that translate to end-of-period pension assets as

$$(23) \quad y_{p,t} = m_{p,t} + \chi(c_{p,t})$$

where χ is a function representing the incentives to make a pension contribution, with $\chi(x) = 1 + \bar{\chi} \log(1 + x)$, $\bar{\chi} > 0$. Finally, employment status evolves according to $z_{t+1} = d_t z_t$ and so, a retired agent cannot work again.

The feasibility correspondence for the problem Γ_t , is given by (i) the borrowing constraint on assets $y_t \geq 0$, (ii) the liquidity constraint preventing pension withdrawals before retirement

$$(24) \quad \chi^{-1}(y_{p,t} - m_{p,t}) \geq 0$$

and (iii) the constraint preventing retirees from making further pension contributions

$$(25) \quad y_{p,t}(1 - z_t) = 0$$

Turning to payoffs, the agent enjoys consumption according to a CRRA utility function with parameter $\rho > 1$, and discounts time according to a factor $\beta \in (0, 1)$. An agent who decides to remain employed pays a utility cost $\delta > 0$. Thus, the Bellman equation for a worker who chooses to continue working becomes³⁶

$$(26) \quad v_t^1(w_t, 1, m_{f,t}, m_{p,t}) = \max_{y_t \in \Gamma_t(x_t)} \left\{ \frac{c_t^{\rho-1}}{\rho-1} + \beta \mathbb{E}_{x_t} [v_{t+1}(w_{t+1}, 1, m_{f,t+1}, m_{p,t+1})] \right\} - \delta$$

where $c_t = m_{f,t} - y_{f,t} - c_{p,t}$. In contrast, the Bellman equation for a worker who chooses to retire next period becomes

$$(27) \quad v_t^0(w_t, 1, m_{f,t}, m_{p,t}) = \max_{y_t \in \Gamma_t(x_t)} \left\{ \frac{c_t^{\rho-1}}{\rho-1} + \beta \mathbb{E}_{x_t} [v_{t+1}(0, m_{f,t+1})] \right\}$$

where $c_t = m_{f,t} - y_{f,t} - c_{p,t}$. (To emphasise the distinction between those who continue working and those who choose to retire, we have written each individual state variable as an argument for the value function through a slight abuse of the notation we have established.)

The optimal discrete choice each period is $d_t = \arg \max_{d \in \{0,1\}} v_t^d(w_t, 1, m_{f,t}, m_{p,t})$. The decision problem for the retiree is thus to solve a standard perfect foresight consumption-saving problem; we omit the retiree Bellman equations for brevity (Druehl and Jørgensen, 2017).

5.1.1. Necessary Euler equation. The utility function in this application will be unbounded below since the state space of the liquid assets is \mathbb{R}_+ . If the agent arrives into a period with state $m_{f,t} > 0$, then for $\Gamma_t(x_t)$ to be compact-valued, $\Gamma_t(x_t)$ must include the feasible choice of zero consumption where utility hits $-\infty$. On the other hand, if we exclude zero consumption from the feasible choices given x_t , then $\Gamma_t(x_t)$ will not be compact-valued. Thus, even without the issue of non-differentiability due to discrete choices, the generalized results by Rincón-Zapatero and Santos (2009) cannot be directly applied to derive the Euler equation. Moreover, the solution will not always be an interior point in $\Gamma_t(x_t) \cap \Gamma_t^{-1}(y_{t+1})$ since a worker may not make pension contributions in one or more consecutive periods. Thus, the Clausen and Strub (2020) results cannot be applied either, as the pension withdrawal constraint (25) may bind in consecutive periods.³⁷ However, it is straightforward to verify that Assumptions D.1 - D.3 hold (see online appendix).

In terms of the general setup of Section 2.2, note that $u_t(w_t, z_t, m_t, d_t, y_t) = \beta^t \frac{c_t^{\rho-1}}{\rho-1} =: \beta^t \varphi_u(c_t)$. We can now use the S-function to derive the necessary Euler equations. In particular, at time t ,

³⁶Recall our discussion of current period discrete choice-specific value functions in Section 2.3.1.

³⁷If we additionally impose the risk of zero income, application-specific approaches such as Li and Stachurski (2014) and Ma et al. (2022) also fail since there will be no strictly positive upper bound on the marginal utility of consumption (Carroll and Shanker, 2024).

the FOCs of the S-function are³⁸

$$(28) \quad \varphi'_u(c_t) = \mu_{f,t} + \beta \mathbb{E}_{x_t} [u'_{t+1}(c_{t+1}) (1 + r_f)] = \mu_{f,t} + \beta \mathbb{E}_{x_t} \lambda_{t+1,f} (1 + r_f)$$

$$(29) \quad \varphi'_u(c_t) = \mu_{p,t} + \mathbb{E}_{x_t} \lambda_{p,t+1} (1 + r_p) (1 + \chi'(c_{p,t}))$$

$$(30) \quad \mu_{f,t} y_{f,t} = 0$$

$$(31) \quad \mu_{p,t} c_{p,t} = 0$$

$$(32) \quad \lambda_{p,t} = z_t \mathbb{E}_{x_t} \lambda_{p,t+1} (1 + r_p) + (1 - z_t) \varphi'_u(c_t)$$

$$(33) \quad \lambda_f = \varphi'_u(c_t)$$

where we have $c_t = m_{f,t} - y_{f,t} - c_{p,t}$ and $c_{p,t} = y_{p,t} - m_{p,t} - \chi(c_{p,t})$.

The model will have four constrained regions defined using $y_t \geq 0$ and (24). We follow Druedahl and Jørgensen (2017) and label these regions by $\text{IB} = \{\text{ucon}, \text{dcon}, \text{acon}, \text{con}\}$. Following the steps (A)- (C) below Theorem 2, we can construct each region, its corresponding exogenous variables and the projected Euler equation as follows:

- **ucon** indexes the region where none of the constraints bind – $K_{\text{ucon},t}^A = \{a_t | y_{f,t} \geq 0, y_{p,t} \geq 0, \mu_t = 0\}$, with exogenous variables $y_{f,t}$ and $y_{p,t}$, and projected Euler equation $\pi_Y \mathbf{E}_{a,t}$ given by (28) and (29),
- **dcon** indexes the region where the pension constraint (24) binds – $K_{\text{dcon},t}^A = \{a_t | y_{f,t} > 0, y_{p,t} = m_{p,t}, \mu_{f,t} = 0, \mu_{p,t} \geq 0, m_{p,t} \in M_{p,t}\}$, with exogenous variables $y_{f,t}$ and $y_{p,t}$, and $\pi_Y \mathbf{E}_{a,t}$ given by (28) and (31),
- **acon** indexes the region where the financial asset borrowing constraint ($y_{f,t} \geq 0$) binds – $K_{\text{acon},t}^A = \{a_t | y_{f,t} = 0, y_{p,t} \geq 0, \mu_{f,t} \geq 0, \mu_{p,t} = 0\}$, with exogenous variables $\mu_{f,t}$ and $y_{p,t}$, and $\pi_Y \mathbf{E}_{a,t}$ given by (29) and (30), and
- **con** indexes the region where all the constraints bind – $K_{\text{con},t}^A = \{a_t | y_{f,t} = 0, y_{p,t} \geq m_{p,t}, \mu_{f,t} \geq 0, \mu_{p,t} = 0\}$, with exogenous variables $\mu_{f,t}$ and $\mu_{p,t}$, and $\pi_Y \mathbf{E}_{a,t}$ given by (30) and (31).

In the online appendix we verify that by Theorem 2 and Proposition 2, we can construct an exogenous grid \mathcal{A}_t in any two-dimensional regions above. By selecting only points in these regions that satisfy complementary slackness, we avoid having to compute each constrained policy separately over the full exogenous grid. In practice, the exogenous grid where $\mu_{f,t}$ is the exogenous variable can be constructed as points of consumption c_t . The exogenous grid where $\mu_{p,t}$ is the exogenous variable can be constructed as points of end-of-period pension assets $y_{p,t}$.

Next, we can choose consumption and end-of-period pension assets evaluated at the exogenous grid for the corresponding endogenous grid point, denoted by $m \mapsto (\acute{c}_t(m), \acute{y}_{p,t}(m))$, as the grid

³⁸We write the shadow values and multipliers in their current value form below.

distance function κ_t . It is straightforward to show that both consumption and pension post-state policy functions given a future sequence of discrete choices \vec{d}_{t+1} , $c_t^{\vec{d}_{t+1}}$, and $y_{p,t}^{\vec{d}_{t+1}}$ are monotone and bi-Lipshitz, and have a Lipshitz constant L no greater than 1 (see online appendix where we verify that Assumptions E.1- E.3 hold). This allows us to set the jump detection threshold to $\bar{J} > 1$. We can thus apply EGM and RFC algorithm to the grid \mathcal{A}_t to approximate the time t policy functions $(y_{f,t}, y_{p,t})$. Once the policy functions are approximated, λ_t can be approximated using (11).

Proposition 2. *For each t , the policy functions y_t^d are Lipshitz with Lipshitz constant $L \leq 1$.*

5.1.2. *Numerical implementation.* We now illustrate the RFC algorithm for the retirement choice model above, using the baseline calibrations in Druedahl and Jørgensen (2017). To benchmark our method, we implement the solution algorithm using (i) the nested EGM suggested by Druedahl (2021) (‘NEGM’ henceforth), (ii) EGM using our RFC algorithm and a Delaunay triangulation (‘RFC w. Delaunay’ henceforth),³⁹ and (iii) EGM using the upper envelope method in Druedahl and Jørgensen (2017) (‘G2EGM’ henceforth). To implement RFC efficiently, we apply the vectorized algorithm iteratively to nearest neighbours of a subset of total points in the endogenous grid until no new sub-optimal points are found.

Figure 3 shows the constrained segments from the set IB within both the endogenous and exogenous grid at time $t = T - 13$. Each region of the exogenous grid on the RHS panel is a two-dimensional sub-manifold of the space of observable variables, defined by the sets $K_{i,t}$.⁴⁰ The sub-optimal points noted in the figure are points within the regions that are removed by the RFC algorithm. Our contribution in Theorem 2 showed that inverting from these regions leads to the optimal solution. The power of Theorem 2 is thus demonstrated here by the isomorphic mapping of each segment from the RHS panel to the corresponding region in the endogenous grid in the LHS panel. Note that while different constrained regions overlap in the exogenous grid, they form disjoint segments in the endogenous grid – i.e., each point in the endogenous grid is associated with a unique optimal solution and a optimal constraint choice. In terms of computational speed, Figure 4 shows the time it takes to solve the model for 20 periods. We note that the RFC implementation and the upper envelope method are comparable in terms of time efficiency, and both are about twice as fast as NEGM. The gain in speed due to the vectorized RFC and calculating the optimal constraints from the exogenous grid also allows us to use an ‘off-the shelf’ SciPy implementation of Delaunay triangulation to interpolate over the endogenous grid, thereby significantly simplifying the implementation of the EGM for the model. Turning finally to computational accuracy, we find the RFC implementation continues to be comparable to the upper envelope method in this respect, and even dominates slightly on the mean Euler error (see online appendix). Interestingly, the distribution of the Euler errors obtained from the RFC algorithm has a notably lower kurtosis compared to the one of G2EGM errors (2.56 vs. 3.45). This can also be seen in Figure 5 that plots the histogram of errors for the two methods.

³⁹In implementing the EGM step for the RFC algorithm, we use the Euler equations defined above to identify the binding constraints from the exogenous grid.

⁴⁰This manifold is isomorphic to the regions in Figure 3 defined over consumption and end-of-period pension assets.

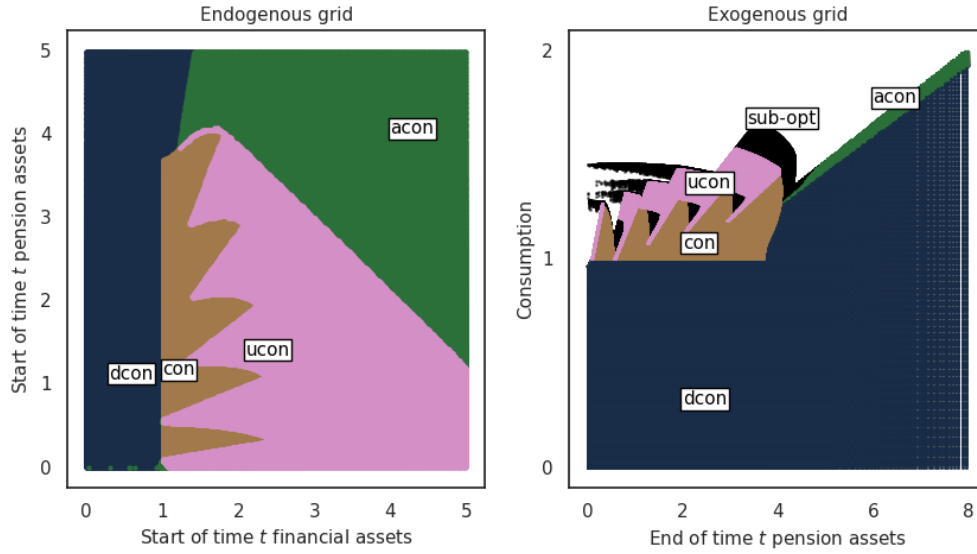


Figure 3. Constrained regions under the EGM

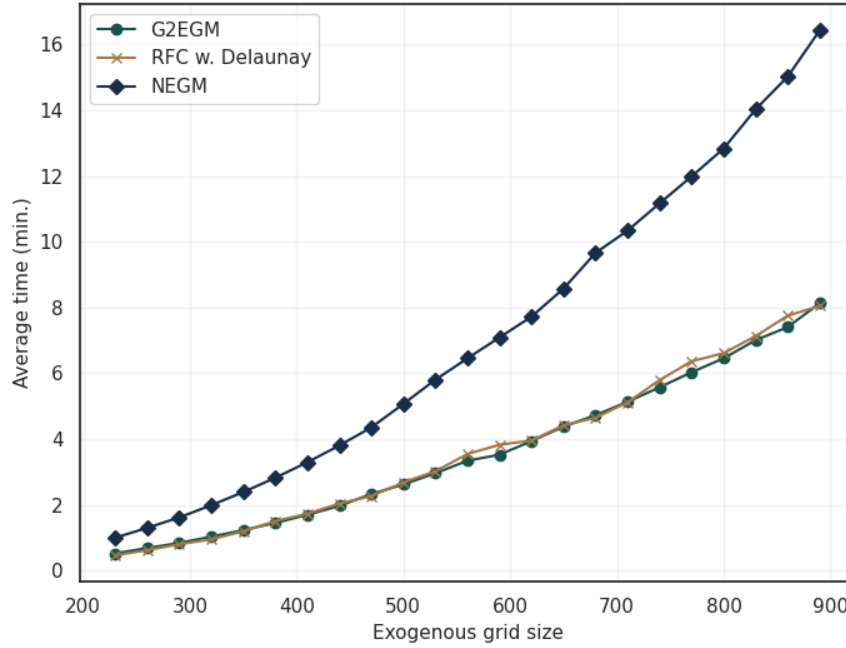


Figure 4. Computational speed benchmarking

5.2. Application 2: Housing investments with adjustment friction. We now turn to demonstrating our results in the stylized version of a veritable workhorse in the housing frictions literature (Kaplan and Violante, 2014; Yogo, 2016; Dobrescu et al., 2022). To do so while maintaining comparability, our model specification closely follows Druedahl (2021). Interestingly, while the example

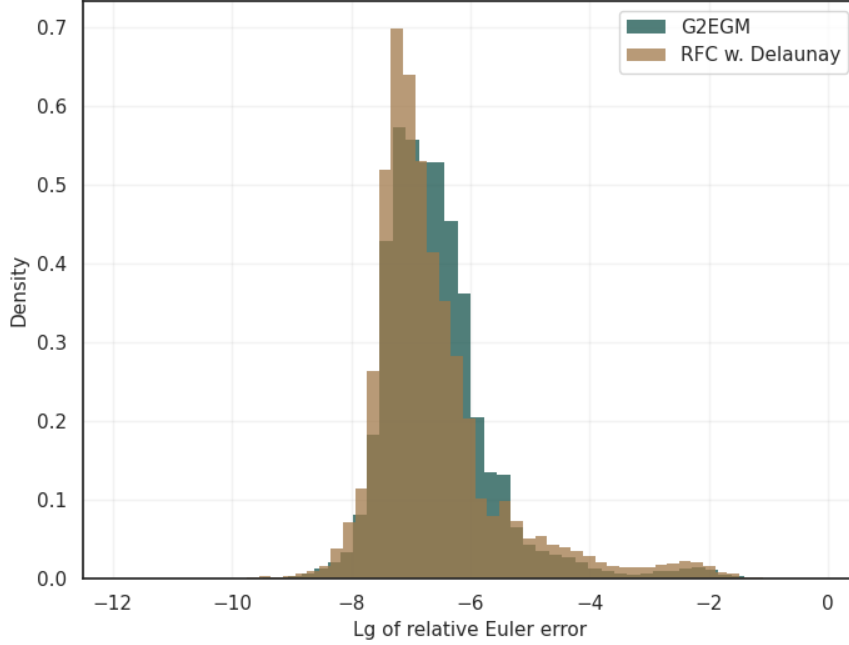


Figure 5. Euler error benchmarking

in this section also features two dimensions of savings – one for liquid (financial) assets and one for illiquid (housing) assets – pure EGM cannot be applied. Rather, optimal financial and housing assets occupy a one-dimensional sub-manifold of the post-state space. We show EGM can still be employed to gain significant speed and numerical accuracy, using a root-finding step to construct an exogenous grid.

5.2.1. Model environment. Let T be finite. Consider an agent who chooses a post-state $y_t = (y_{f,t}, y_{h,t})$ consisting of end-of-period financial assets $y_{f,t}$ and housing assets $y_{h,t}$. The continuous state variables for the problem are start-of-period financial assets $m_{f,t}$ and housing assets $m_{h,t}$. Thus, the post-state space is $Y_t = Y_{f,t} \times Y_{h,t} = \mathbb{R}_+^2$, and the continuous state space is $M_t = M_{f,t} \times M_{h,t} = \mathbb{R}_+^2$. The agent also makes a discrete choice d_t , where investing in and out of housing stock can only be made if $d_t = 1$. Otherwise, if $d_t = 0$ then $y_{h,t+1} = m_{h,t+1}$, and we must have

$$(34) \quad (y_{h,t} - m_{h,t})(1 - d_t) = 0$$

Investments can be made in and out of the stock of $m_{f,t}$ without friction. Turning to the transition functions, note that the financial asset state evolves according to

$$(35) \quad m_{f,t+1} = (1 + r)y_{f,t} + w_{t+1}$$

where financial assets earn a rate of return r , and w_{t+1} is a stochastic wage. We assume that housing earns no returns and so,

$$(36) \quad m_{h,t+1} = y_{h,t+1}$$

and that the equations describing the non-negativity constraint $y_t \geq 0$ and the friction on housing $(y_{h,t} - m_{h,t})(1 - d_t) = 0$ define the value of the feasibility correspondence $\Gamma_t(x_t)$.

Turning to per-period rewards, the agent enjoys utility from non-housing consumption c_t and from the end-of-period housing stock $y_{h,t}$. We assume per-period rewards given by the function⁴¹

$$(37) \quad u_t(m_t, y_t) = \beta^t \underbrace{\left[\frac{c_t^{\rho-1} - 1}{\rho - 1} + (1 - \alpha) \ln(y_{h,t}) \right]}_{:= \varphi^u(c_t, y_{h,t})}$$

where consumption satisfies

$$(38) \quad c_t = m_{f,t} + d_t m_{h,t} - y_{a,t+1} - d_t(1 + \tau)y_{h,t+1}$$

Adjusting the housing stock to a value $y_{h,t}$ requires a payment of $\tau y_{h,t}$ with $\tau > 0$, leading to a non-concave continuation value.

Turning to the agent's recursive problem, the Bellman equation for an agent who decides not to adjust their housing stock becomes

$$(39) \quad v_{0,t}(w_t, m_t) = \max_{y_t \in \Gamma_t(x_t)} \{ \varphi_t^u(c_t, y_{h,t}) + \beta \mathbb{E}_{x_t} v_{t+1}(w_{t+1}, m_{a,t+1}, m_{h,t}) \}$$

where $c_t = m_{f,t} - y_{f,t}$. (To emphasize the distinction between adjusters and non-adjusters, we have written each state variable as an argument for the value function through a slight abuse of the notation we have established.) The Bellman equation for an agent adjusting their housing stock is

$$(40) \quad v_{1,t}(w_t, m_{f,t}, m_{h,t}) = \max_{y_t \in \Gamma_t(x_t)} \{ \varphi_t^u(c_t, y_{h,t}) + \beta \mathbb{E}_{x_t} v_{t+1}(w_{t+1}, m_{a,t+1}, m_{h,t+1}) \}$$

where $c_t = m_{f,t} + m_{h,t} - y_{f,t} - (1 + \tau)y_{h,t+1}$. For both Bellman equations, (35), (36) and (38) must hold. The optimal discrete choice each period is $d_t = \arg \max_{d \in \{0,1\}} v_t^d(w_t, m_{f,t}, m_{h,t})$ and

$$(41) \quad v_t(w_t, m_{f,t}, m_{h,t}) = \max_{d \in \{0,1\}} v_t^d(w_t, m_{f,t}, m_{h,t})$$

5.2.2. Necessary Euler equations. For periods prior to the terminal one, the recursive Euler equation **(EO2)** for financial assets is

$$(42) \quad \partial_c \varphi^u(c_t, y_{h,t}) = \mu_{a,t} + \beta \mathbb{E}_{x_t} \Lambda_{a,t+1}(w_{t+1}, m_{f,t+1}, m_{h,t+1}) \geq \beta(1 + r) \mathbb{E}_{x_t} \partial_c \varphi^u(c_{t+1} y_{h,t+1}),$$

where c_t and c_{t+1} obeys (38), and the state transition equations (35) and (36) hold. Note also that in the last term in (42), the optimal $t+1$ period policy function is $y_{t+1} = y_{t+1}(w_{t+1}, m_{f,t+1}, m_{h,t+1})$.

⁴¹To ease exposition, in what follows we assume that utility from housing and non-durable consumption is separable. A constant elasticity of substitution (CES) specification of consumption and housing is computationally straightforward to implement, and an example is provided in our online repository.

If $d_t = 1$, the recursive Euler equation for housing stock is

$$(43) \quad (1 + \tau) \partial_c \varphi^u(c_t, y_{h,t}) = \mu_{h,t} + \mathbb{E}_{x_t} \Lambda_{h,t+1}(w_{t+1}, m_{f,t+1}, m_{h,t+1}) + \partial_h \varphi^u(c_t, y_{h,t})$$

$$\geq \underbrace{\mathbb{E}_{x_t} \sum_{k=t}^{\iota-1} \beta^{t-\iota} \partial_{y_h} \varphi^u(c_k, y_{h,k+1})}_{\text{Marginal value of housing services}} + \underbrace{\mathbb{E}_{x_t} \beta^{t-\iota} (\partial_c \varphi^u(c_\iota, y_{h,\iota+1}))}_{\text{Marginal value of liquidating housing at time } \iota}.$$

The intuition of the financial assets Euler equation (42) is standard. The housing Euler equation (43), however, features a stochastic time subscript ι defined as the next period when $d_\iota = 1$. Since the next time the stock is adjusted will be stochastic, ι becomes a random stopping time. Equation (43) then tells us that the shadow value of the housing stock is the discounted expected value of the stock *when the stock is next liquidated*, along with the stream of housing services provided up to the time of liquidation. (See Section 4.1 in Kaplan and Violante (2014) for a similar intuition.)

Remark 7. *If the probability that $\iota > t + 1$ is non-zero, then at time $t + 1$, there is a realization where $d_{t+1} = 0$ and $d_{t+1}, y_{t+1} \in \Gamma_{t+1}(x_{t+1})$ if and only if $y_{h,t+1} = m_{h,t+1}$ and thus $y_{h,t}$ cannot be in the interior of the set $\{y \mid d_{t+1}, y_{t+1} \in \Gamma_{t+1}(F_t^m(d_t, y, w_{t+1}))\}$. Thus, Theorem 6 by Clausen and Strub (2020) cannot be applied since the interiority assumption on next period policy in the one-shot deviation problem is violated.*

Once we find the time t solution (by following the steps below), let $y_{f,d,t}$ and $y_{h,d,t}$ denote the optimal choice-specific policy functions conditional on the time t discrete choice, with $d \in \{0, 1\}$. Given the optimal policy functions, the iteration of the shadow values is

$$(44) \quad \Lambda_{h,t}(x_t) = d_t(x_t) \partial_c \varphi^u(c_t, y_{h,t}) + \beta \mathbb{E}_{x_t} (1 - d_t(x_t)) [\mathbb{E}_{x_t} \Lambda_{h,t+1}(x_{t+1}) + \partial_{y_h} \varphi^u(c_t, y_{h,t})], \text{ and}$$

$$(45) \quad \Lambda_{a,t}(x_t) = \partial_{y_h} \varphi^u(c_t, y_{h,t})$$

where $x_t = (w_t, m_{f,t}, m_{h,t})$, and

$$(46) \quad c_t = m_{f,t} + d_t(x_t) m_{h,t} - d_t(x_t) y_{a,d_t(x_t),t}(x_t) - y_{h,d_t(x_t),t}(x_t) (1 + \tau)$$

$$(47) \quad y_{h,t} = y_{h,d_t(x_t),t}(x_t).$$

5.2.3. Computation using EGM and the RFC algorithm. Suppose we know v_{t+1} and $\Lambda_{h,t+1}$. We can first apply standard EGM with the RFC algorithm to evaluate $y_{f,0,t}$ for *non-adjusters*, since only one Euler equation - i.e., equation (42) - will hold. For each possible time t housing state $m_{h,t}$ in the housing grid $\mathcal{Y}_{h,t}$ and exogenous state w_t , we can approximate $y_{f,0,t}(w_t, \cdot, m_{h,t})$ by first setting an exogenous grid (over the constrained and unconstrained regions) of $y_{f,t}$ and $\mu_{f,t}$ values (holding $y_{h,t} = m_{h,t}$ fixed as no adjustment occurs), and then creating an endogenous grid of time t financial assets using (42) and budget constraint (38). The RFC algorithm can then be applied to eliminate sub-optimal points, allowing us to obtain an approximation of the policy function $y_{f,0,t}$.

We now turn to *adjusters*. Bellman equation (40) shows that the solution for adjusters only depends on ‘total’ resources $\bar{m}_t = m_{f,t} + m_{h,t}$. Thus, the dimension of the active state space \mathbb{R}_+ (i.e., one) is less than the dimensions of the post-states (i.e., two). By Theorem 2, the recursive Euler equation for adjusters cannot be inverted on the post-state space. By Proposition 3, there will then be a one-dimensional sub-manifold embedded in the post-state space from which the adjuster Euler equations can be inverted (see online appendix for details). The sub-manifold will thus be characterized by financial and housing asset values that satisfy the Euler equation. To construct the exogenous grid, note we can evaluate time t consumption c_t , given the values of $y_{h,t}$ and $y_{f,t}$, as

$$(48) \quad c_t = \partial_c \varphi^{u,-1}((1+r)\beta \Lambda_{f,t+1}(m_{f,t+1}, m_{h,t+1}), y_{h,t})$$

where $\partial_c \varphi^{u,-1}$ is the analytical inverse of $\partial_c \varphi^u$ in its first argument. The procedure to evaluate the policy functions for adjusters is then as follows:

Box 2: RFC and EGM for the adjuster policy function

- (1) Fix ξ_t and a uniform grid over values of the exogenous variable $y_{h,t}$, $\mathcal{Y}_{h,t}$. Initialise the exogenous grid as an empty array (\mathcal{A}_t), current period objective values (\mathcal{V}_t), and an endogenous wealth grid (\mathcal{M}_t).
- (2) For each $y_{h,t,i}^\# \in \mathcal{Y}_{h,t}$:
 - (i) Evaluate the P multiple roots to (43) in terms of $y_{f,t}$, with c_t evaluated by (48), and $y_{h,t}$ fixed as $y_{h,t,i}^\#$. Collect the roots in a tuple $(y_{f,t,i_0}^\#, \dots, y_{f,t,i_j}^\#, y_{f,t,i_P}^\#)$. Append the tuples $((y_{f,t,i_0}^\#, y_{h,t,i}^\#), \dots, (y_{f,t,i_P}^\#, y_{h,t,i}^\#))$ to \mathcal{A}_t .
 - (ii) For each root in $(y_{f,t,0}^\#, \dots, y_{f,t,i_j}^\#, \dots, y_{f,t,i_P}^\#)$, evaluate the endogenous grid points of total resources $(\bar{m}_{t,0}^\#, \dots, \bar{m}_{t,j}^\#, \dots, \bar{m}_{t,P}^\#)$ using the budget constraint

$$\bar{m}_{t,i_j}^\# = y_{f,t,i_j}^\# + (1+\tau)y_{h,t,i}^\# + c_t$$

and evaluate the current period objective values $(v_{t,0}^\#, \dots, v_{t,i_j}^\#, \dots, v_{t,i_P}^\#)$ as

$$v_{t,i_j}^\# = u(c_t, y_{h,t,i}^\#) + \beta \mathbb{E}_{w_t} v_{t+1}(w_{t+1}, (1+r)y_{f,t,i_j}^\#, y_{h,t,i}^\#)$$

- (iii) Append the P endogenous grid points to $(\bar{m}_{t,0}^\#, \dots, \bar{m}_{t,j}^\#, \dots, \bar{m}_{t,P}^\#)$ to \mathcal{M}_t , and the time t objective values $(v_{t,0}^\#, \dots, v_{t,i_j}^\#, \dots, v_{t,i_P}^\#)$ to \mathcal{V}_t .
- (3) Apply the RFC algorithm to the grids \mathcal{V}_t , \mathcal{A}_t , and \mathcal{M}_t to recover the refined endogenous grid points \mathcal{M}_t^* , value grid \mathcal{V}_t^* , and end-of-period state (policy) grid \mathcal{Y}_t^* .

We apply the above steps to each w_t in the exogenous shock grid. With $y_{h,1,t}$ and $y_{f,1,t}$ approximated on a uniform grid, we can then construct $y_{h,t}$ and $y_{f,t}$ in the standard way by solving (41).

Finally, note that the endogenous grid points \mathcal{M}_t will not be monotone in end-of-period housing (Figure (6)). This is because as agents become wealthier, they will reach a threshold where they anticipate upgrading their housing stock sometimes in the future. At this threshold, they also expect to discontinuously decrease future non-housing consumption, causing a jump up in the RHS of (43). As a result, they will discontinuously decrease current period housing consumption. This

non-monotonicity means existing upper envelope methods (Iskhakov et al., 2017) cannot be applied. Moreover, the optimal housing policy that takes into account the future sequence of adjustment decisions will be non-monotone. Nonetheless, fixing a future sequence of discrete choices, we can verify that housing consumption and financial assets are monotone (see online appendix) and satisfy a Lipschitz bound of 1, allowing us to set $\bar{J} = 1$. We can also set end-of-period pension assets evaluated at the exogenous grid for the corresponding endogenous grid point $m \mapsto \dot{y}_{h,t}(m)$ as the grid distance function $\dot{\kappa}_t$ that we can use to detect RFC jumps for adjusters. Similarly for non-adjusters, we can set consumption $m \mapsto \dot{y}_{h,t}(m)$ as the grid distance function $\dot{\kappa}_t$.

5.2.4. Numerical implementation. To parameterize the model, we set $\rho = 3$, $\alpha = 0.66$, $\beta = .93$, $\tau = .18$, $r = 0.01$, and $T = 60$. We assume \tilde{w}_t is the wage function for females in Dobrescu et al. (2018), with $w_t = \tilde{w}_t(\tilde{z})$ and $\tilde{\eta}$ being a random variable taking values in $\{0.1, 1\}$ with equal probability; for simplicity, wage shocks are i.i.d. To benchmark our method with the others, we will implement the solution algorithm using VFI, EGM with our RFC algorithm, and the nested EGM method in Druedahl (2021). As the financial assets and total resources grids are one-dimensional, we use standard linear interpolation to implement all methods. To implement RFC, when the endogenous grid is one-dimensional, we find it is more efficient to proceed sequentially instead of computing the tangent plane between each point and its neighbours. In particular, we proceed from the lowest endogenous grid point $m_{0,t}^\#$ and apply RFC to the neighbouring point $m_{1,t}^\#$. If $m_{1,t}^\#$ is sub-optimal, we delete the point and test $m_{2,t}^\#$ from $m_{0,t}^\#$. If $m_{1,t}^\#$ point is optimal, we move to $m_{1,t}^\#$ and apply RFC to test $m_{2,t}^\#$. The procedure is repeated until all sub-optimal points are removed.⁴²

Figure 6 shows the map of endogenous grid points to the exogenous grid for a 59 year old, with the exogenous grid points belonging to a subset of a collection of one-dimensional spaces, each corresponding to a particular future sequence of discrete choices. Despite the irregular grid and non-monotonicity of the optimal policy, Figure 7 shows how the RFC algorithm recovers the optimal points by zooming in on the top RH section of the exogenous grid. Figure 8 then compares computational speed, and shows that despite the intermediate root-finding step, EGM with RFC (i) still outperforms VFI by a factor of more than 20, and (ii) is comparable in scale with NEGM but still 25% faster. As expected, since EGM with root finding uses all the information contained the Euler equation to compute the optimal policy, Figure 9 shows that our RFC algorithm delivers up to an order of magnitude improvement in accuracy over both VFI and NEGM.

⁴²Our online repository contains implementations of both the sequential and non-sequential versions.

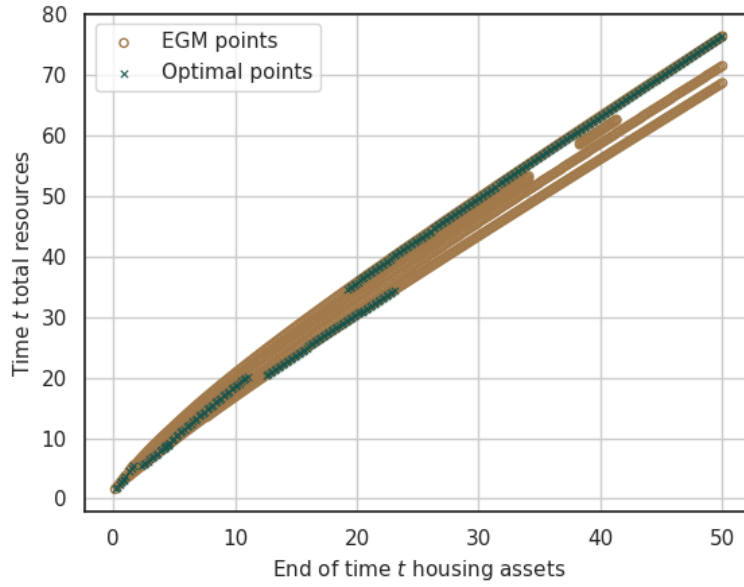


Figure 6. Endogenous total resources plotted on an exogenous grid

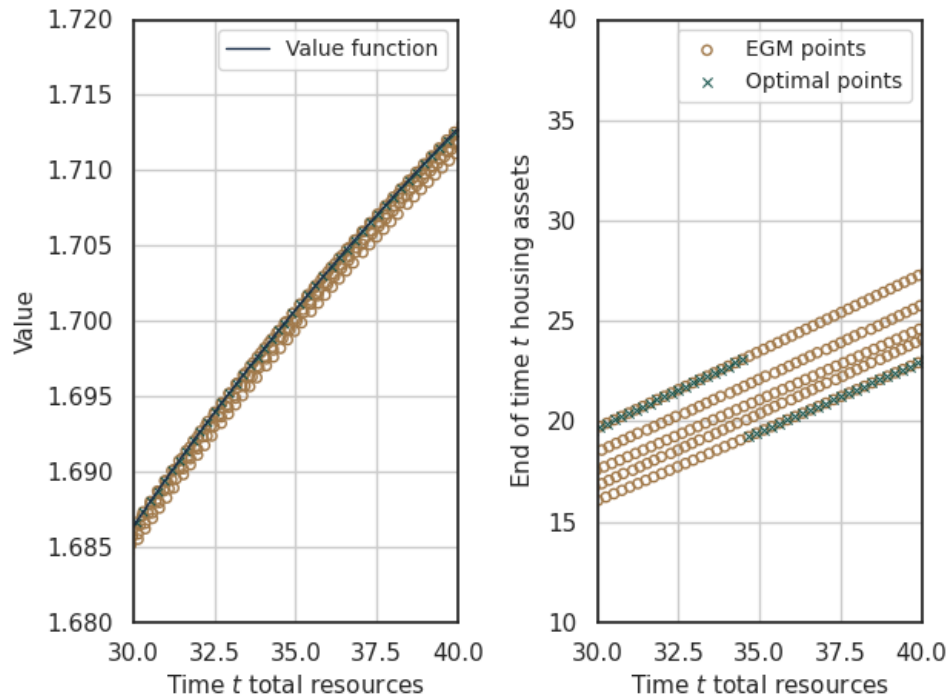


Figure 7. Value function and optimal housing policy function for the top RH section of the endogenous grid

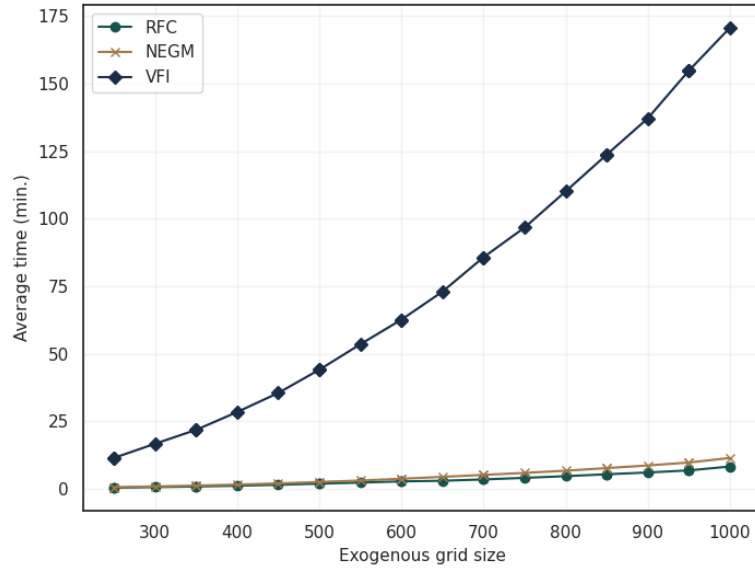


Figure 8. Computational speed benchmarking

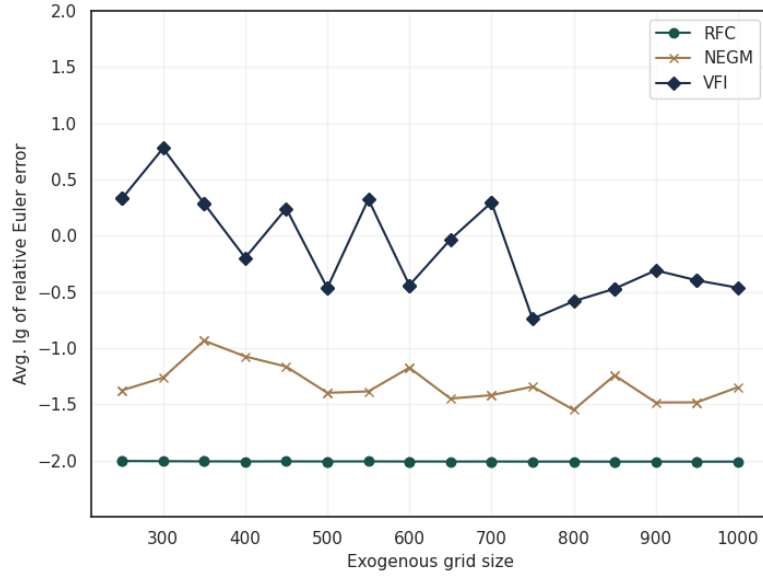


Figure 9. Euler error benchmarking

6. CONCLUSIONS

This study addresses several critical challenges in applying dynamic programming methods to solve high-dimensional optimization models with discrete-continuous choices. Our contribution enables a rigorous and systematic implementation of the EGM to maximize the use of first order information to solve such models efficiently. In particular, by introducing the S-function, we establish a general and straightforward way to derive necessary FOCs (Euler equations) in all classes of models with non-compact feasibility correspondences, unbounded reward, occasionally binding constraints, and discrete choices. We are also the first to provide verifiable conditions on the model primitives that determine when the EGM is well-defined. Additionally, our RFC algorithm offers a highly efficient and accurate avenue to solve discrete-continuous problems. This algorithm is not only compatible with vectorized, high-performance computing but also introduces verifiable error bounds for the EGM. We finally demonstrate the practical impact of our contributions via two workhorse economics applications, with a special focus on the RFC gains in computational speed and accuracy, as well as the ability of our approach to handle multidimensional problems that could not be previously solved using EGM.

One topic we plan to tackle next concerns introducing model uncertainty in the definition of the inverse optimization problems we have used to characterize the EGM. Our setup so far assumed the exogenous grid was observed ‘as if’ it was the result of a model-consistent behaviour given the deeper structural parameters. However, the current literature on inverse optimization incorporates various methods to minimize the uncertainty related to observed variables being model-consistent (Bertsimas et al., 2015; Ghobadi et al., 2018; Chan et al., 2023). Understanding the implications of these advancements in inverse optimization for dynamic structural estimation is a key area of further work.

REFERENCES

- Arellano, C., Maliar, L., Maliar, S., and Tsyrennikov, V. (2016). Envelope condition method with an application to default risk models. *Journal of Economic Dynamics and Control*, 69:436–459.
- Attanasio, O., Levell, P., Low, H., and Sanchez-Marcos, V. (2018). Aggregating elasticities: Intensive and extensive margins of women’s labor supply. *Econometrica*, 86(6):2049–2082.
- Auclert, A., Bardóczy, B., Rognlie, M., and Straub, L. (2021). Using the sequence-space jacobian to solve and estimate heterogeneous-agent models. *Econometrica*, 89(5):2511–2547. Citations: 25.
- Bertsekas, D. (2022). *Abstract dynamic programming*. Athena Scientific.
- Bertsimas, D., Gupta, V., and Paschalidis, I. C. (2015). Data-driven estimation in equilibrium using inverse optimization. *Mathematical Programming*, 153(2):595–633.
- Bewley, T. F. (1972). Existence of equilibria in economies with infinitely many commodities. *Journal of Economic Theory*, 4(3).
- Borovkov, A. A. (2013). *Stochastic recursive sequences*, pages 507–526. Springer London, London.

- Brumm, J. and Scheidegger, S. (2017). Using Adaptive Sparse Grids to Solve High-Dimensional Dynamic Models. *Econometrica*, 85(5):1575–1612.
- Cao, D. (2020). Recursive equilibrium in Krusell and Smith (1998). *Journal of Economic Theory*, 186:104978.
- Carroll, C. D. (2006). The method of endogenous gridpoints for solving dynamic stochastic optimization problems. *Economics Letters*, 91(3):312–320.
- Carroll, C. D. and Shanker, A. (2024). Theoretical Foundations of Buffer Stock Saving. *Working paper*.
- Chan, T. C. Y., Mahmood, R., and Zhu, I. Y. (2023). Inverse optimization: Theory and applications. *Operations Research*, Preprint(Preprint):Preprint.
- Chen, L. and Xu, J.-c. (2004). Optimal Delauny triangulations. *Journal of Computational Mathematics*, 22(2):299–308.
- Clausen, A. and Strub, C. (2020). Reverse calculus and nested optimization. *Journal of Economic Theory*, 187.
- Coleman, W. J. (1990). Solving the stochastic growth model by policy-function iteration. *Journal of Business and Economic Statistics*, 8(1):27–29.
- Cooper, I. (2006). Asset pricing implications of nonconvex adjustment costs and irreversibility of investment. *Journal of Finance*, 61(1):139–170.
- Cosar, A. K. and Green, E. J. (2014). Necessary and sufficient conditions for dynamic optimization. *Macroeconomic Dynamics*, FirstView:1–18.
- Dávila, J., Hong, J. H., Krusell, P., and Ríos-Rull, J.-V. (2012). Constrained Efficiency in the Neoclassical Growth Model With Uninsurable Idiosyncratic Shocks. *Econometrica*, 80(6):2431–2467.
- Deaton, A. (1991). Saving and Liquidity Constraints. *Econometrica*, 59(5):1221.
- Dechert, W. (1982). Lagrange multipliers in infinite horizon discrete time optimal control models. *Journal of Mathematical Economics*, 9:285–302.
- Dobrescu, L. I., Fan, X., Bateman, H., Newell, B. R., and Ortmann, A. (2018). Retirement savings: A tale of decisions and defaults. *Economic Journal*, 128:1047–1094.
- Dobrescu, L. I., Shanker, A., Bateman, H., Newell, B. R., and Thorp, S. (2022). Eggs and baskets: Lifecycle portfolio dynamics. *SSRN Working Paper No. 4069226*.
- Druedahl, J. (2021). A guide on solving non-convex consumption-saving models. *Computational Economics*, 58:747–775.
- Druedahl, J. and Jørgensen, T. H. (2017). A general endogenous grid method for multi-dimensional models with non-convexities and constraints. *Journal of Economic Dynamics and Control*, 74:87–107.

- Fagereng, A., Holm, M. B., Natvik, G., and Moll, B. (2019). Saving behavior across the wealth distribution : The importance of capital gains. *NBER Working Paper No. 26588*.
- Feinberg, E. A., Kasyanov, P. O., and Zadoianchuk, N. V. (2012). Average cost Markov decision processes with weakly continuous transition probabilities. *Mathematics of Operations Research*, 37(4):591–607.
- Fella, G. (2014). A generalized endogenous grid method for non-smooth and non-concave problems. *Review of Economic Dynamics*, 17:329–344.
- Ghobadi, K., Lee, T., Mahmoudzadeh, H., and Terekhov, D. (2018). Robust inverse optimization. *Operations Research Letters*, 46(3):339–344.
- Gonzalez-Sanchez, D. and Hernandez-Lerma, O. (2013). *Discrete-time stochastic control and dynamic potential games: The Euler equation approach introduction and summary*. Springer Netherlands.
- González-Sánchez, D. and Hernández-Lerma, O. (2013). On the Euler equation approach to discrete-time nonstationary optimal control problems. *Journal of Dynamics and Games*, 1(1):57–78.
- Harris, C. R., Millman, K. J., van der Walt, S. J., Gommers, R., Virtanen, P., Cournapeau, D., Wieser, E., Taylor, J., Berg, S., Smith, N. J., Kern, R., Picus, M., Hoyer, S., van Kerkwijk, M. H., Brett, M., Haldane, A., del Río, J. F., Wiebe, M., Peterson, P., Gérard-Marchant, P., Sheppard, K., Reddy, T., Weckesser, W., Abbasi, H., Gohlke, C., and Oliphant, T. E. (2020). Array programming with NumPy. *Nature*, 585(7825):357–362.
- Hernandez-Lerma, O. and Lasserre, J. (2012). *Discrete-time Markov control processes: Basic optimality criteria*. Stochastic modelling and applied probability. Springer New York.
- Hull, I. (2015). Approximate dynamic programming with post-decision states as a solution method for dynamic economic models. *Journal of Economic Dynamics and Control*, 55:57–70.
- Iskhakov, F. (2015). Multidimensional endogenous gridpoint method: Solving triangular dynamic stochastic optimization problems without root-finding operations. *Economics Letters*, 135:72–76.
- Iskhakov, F., Jørgensen, T. H., Rust, J., and Schjerning, B. (2017). The endogenous grid method for discrete-continuous dynamic choice models with (or without) taste shocks. *Quantitative Economics*, 8(2):317–365.
- Iyengar, G. and Kang, W. (2005). Inverse conic programming with applications. *Operations Research Letters*, 33(3):319–330.
- Kaplan, G., Mitman, K., and Violante, G. L. (2020). The housing boom and bust: Model meets evidence. *Journal of Political Economy*, 128(9):3285–3345.
- Kaplan, G. and Violante, G. L. (2014). A model of the consumption response to fiscal stimulus payments. *Econometrica*, 82(4):1199–1239.

- Khan, A. and Thomas, J. K. (2008). Idiosyncratic shocks and the role of nonconvexities in plant and aggregate investment dynamics. *Econometrica*, 76(2):395–436.
- Krusell, P. and Smith, A. A. (1998). Income and wealth heterogeneity in the macroeconomy. *Journal of Political Economy*, 106(5):867–896.
- Laibson, D., Maxted, P., and Moll, B. (2021). Present bias amplifies the household balance-sheet channels of macroeconomic policy. *NBER Working Paper No. 29094*.
- Li, H. and Stachurski, J. (2014). Solving the income fluctuation problem with unbounded rewards. *Journal of Economic Dynamics and Control*, 45:353–365.
- Ludwig, A. and Schön, M. (2018). Endogenous grids in higher dimensions: Delaunay interpolation and hybrid methods. *Computational Economics*, 51(3):463–492.
- Lujan, A. (2023). EGMⁿ: The sequential endogenous grid method. *Working paper*.
- Ma, Q., Stachurski, J., and Toda, A. A. (2022). Unbounded dynamic programming via the Q-transform. *Journal of Mathematical Economics*, 100:102652.
- Maliar, L. and Maliar, S. (2013). Envelope condition method versus endogenous grid method for solving dynamic programming problems. *Economics Letters*, 120(2):262–266.
- Maliar, L., Maliar, S., and Winant, P. (2021a). Deep learning for solving dynamic economic models. *Journal of Monetary Economics*, 122:76–101.
- Maliar, L., Maliar, S., and Winant, P. (2021b). Deep learning for solving dynamic economic models. *Journal of Monetary Economics*, 122:76–101.
- Marimon, R. and Werner, J. (2021). The envelope theorem, Euler and Bellman equations, without differentiability. *Journal of Economic Theory*, 196:105309.
- Midrigan, V. (2011). Menu costs, multiproduct firms, and aggregate fluctuations. *Econometrica*, 79(4):1139–1180.
- Reffett, K. L. (1996). Production-based asset pricing in monetary economies with transactions costs. *Economica*, 63(251):427–443.
- Rendahl, P. (2015). Inequality constraints and euler equation-based solution methods. *Economic Journal*, 125(585):1110–1135.
- Rincón-Zapatero, J. P. and Santos, M. S. (2009). Differentiability of the value function without interiority assumptions. *Journal of Economic Theory*, 144(5):1948–1964.
- Rust, J. (1987). Optimal replacement of GMC bus engines: An empirical model of Harold Zurcher. *Econometrica*, 55(5):999–1033.
- Rust, J. (1996). Chapter 14 Numerical dynamic programming in economics. *Handbook of Computational Economics*, 1:619–729.

- Sargent, T. J. and Stachurski, J. (2023). Completely abstract dynamic programming. *Working Paper*, 2308.02148:1–37.
- Sargent, T. J. and Stachurski, J. (2024). Quantitative economics with python using jax: An introduction to jax. https://jax.quantecon.org/jax_intro.html. Accessed: 2024-05-07.
- Shanker, A. (2017). Existence of recursive constrained optima in the heterogenous agent neoclassical growth model. *Working Paper*.
- Skiba, A. K. (1978). Optimal growth with a convex-concave production function. *Econometrica*, 46(3):527–539.
- Sorger, G. (2015). *Dynamic economic analysis: Deterministic models in discrete time*. Cambridge University Press.
- Stachurski, J. (2022). *Economic dynamics: Theory and computation, second edition*. MIT Press.
- White, M. (2015). The method of endogenous gridpoints in theory and practice. *Journal of Economic Dynamics and Control*, 60:26–41.
- Yogo, M. (2016). Portfolio choice in retirement: Health risk and the demand for annuities, housing, and risky assets. *Journal of Monetary Economics*, 80:17–34.